Evolution, 2024, **XX(XX)**, 1–19
https://doi.org/10.1093/evolut/qpae165
Advance access publication 19 November 2024
Original Article

Weak integration allows novel fin shapes and spurs locomotor diversity in reef fishes

Darien R. Satterfield[1], Bernice Yin[1], Sky Jung[1], Samantha Hodges-Lisk[1], Dylan K. Wainwright[2], Michael D. Burns[3], Peter C. Wainwright[1]

[1]Department of Evolution and Ecology, University of California, Davis, United States
[2]Department of Biological Sciences, Purdue University, West Lafayette, United States
[3]Department of Fisheries, Wildlife and Conservation Sciences, Oregon State University, Corvallis, United States
Corresponding author: Department of Evolution and Ecology, 1 Sheilds Ave, University of California, Davis, CA 95616, United States. Email: dsatterfield@fau.edu

Abstract

In functional systems composed of many traits, selection for specialized function can induce trait evolution by acting directly on individual components within the system, or indirectly through networks of trait integration. However, strong integration can also hinder diversification into regions of trait space that are not aligned with axes of covariation among traits. Thus, non-independence among traits may limit functional expansion. We explore this dynamic in the evolution of fin shapes in 106 species from 38 families of coral reef fishes, a polyphyletic assemblage that shows exceptional diversity in locomotor function. Despite expectations of a strong match between form and function, we find subtantial fin shape disparity across species that share a swimming mode. The evolution of fin shape is weakly integrated across the four functionally dominant fins in swimming and integration is weakened as derived swimming modes evolve. The weak integration among fins in the ancestral locomotor condition provides a primary axis of diversification while allowing for off-axis diversification via independent trait responses to selection. However, the evolution of novel locomotor modes coincides with a loss of integration among fins. Our study highlights the need for additional work on the functional consequences of fin shape in fishes.

Keywords: Fin anatomy, evolutionary correlation, functional diversity, locomotion, swimming, macroevolution

Introduction

Locomotor variation is an axis of functional diversity that has direct consequences for ecological diversity, as the locomotor range is generally a limiting factor determining access to resources in an environment (Bellwood & Wainwright, 2001; Citadini et al., 2018; Crumière, 2016; Essner, 2007; Fulton et al., 2001; Granatosky, 2018). In most vertebrate locomotor systems, the ancestral condition is that all limbs work in cooperation to produce movement, creating functional covariation but also commonly showing shared genetic and developmental origins (Gatesy & Dial, 1996; Goswami et al., 2014; Hallgrímsson et al., 2002; Petit et al., 2017; Wimberly et al., 2021). Correlation among morphological units, such as limbs, facilitated by functional, genetic, and developmental linkages can be referred to as morphological integration (Olson & Miller, 1999). Often the functional, genetic, and developmental pathways linking morphological units produce covariation that persists through many generations such that the morphological traits do not evolve independently, known as evolutionary integration (Evans et al., 2023; Klingenberg, 2008; Zelditch & Goswami, 2021).

Within vertebrate clades, the evolution of novel locomotor styles often occurs through the functional decoupling of limb modules. For example, we observe locomotor expansion in mammals associated with the decoupling of fore- and hindlimbs, such as climbing in bipedal marsupials and primates, and flight in bats (Bell et al., 2011; Goswami et al., 2014; Young et al., 2010). Similarly, functional decoupling of the limbs was the necessary precursor for the locomotor expansion from quadrupedal archosaurs to bipedal theropods to avian flight (Gatesy & Dial, 1996; Gatesy & Middleton, 1997). In each case of vertebrate limb decoupling, a reduction of morphological integration between the fore- and hindlimbs relative to quadrupedal ancestors has been observed, which suggests a weakening of shared developmental and genetic pathways that underpin limb correlations (Bell et al., 2011; Garland et al., 2017; Goswami et al., 2014; Kelly & Sears, 2011; Young & Hallgrímsson, 2005; Young et al., 2010). While these studies demonstrate reductions in intraspecific morphological integration when comparing organisms with ancestral locomotor styles and those with broadened locomotor capacities, studies that examine shifts in interspecific limb covariation over deep time scales (evolutionary integration) are rare. However, in birds, as many as three independently evolving locomotor modules (the forelimb, the hind limb, and the tail) have been observed (Eliason et al., 2023; Orkney et al., 2021), providing some evidence of the hypothesized pathway to flight via weakened evolutionary integration among regions of the body that likely evolved with less independence in the quadrupedal theropod ancestors of birds (Gatesy & Dial, 1996; Gatesy & Middleton, 1997).

Received April 8, 2024; revisions received October 7, 2024; accepted November 15, 2024

Associate Editor: Eric Goolsby; Handling Editor: Hélène Morlon

Ray-finned fishes (Actinopterygii), the most species-rich group of vertebrates, have extensive locomotor diversity (Breder, 1926; Lindsey, 1978; Webb, 1984). Numerous classification systems are available to categorize swimming mode in fish; one of the more common methods is identifying the fins used for routine propulsion at average speeds (Supplementary Figure S1; reviewed by Blake, 2004; Breder, 1926; Fulton, 2007; Lindsey, 1978; Sfakiotakis et al., 1999). Many ray-finned fishes swim primarily with the undulation of their body-caudal fin (BCF), while others use the flapping, rowing, or undulation of their median and paired fins (MPF). Within MPF swimming, propulsion can be achieved predominantly by the pectoral fin (labriform) or by the dorsal and anal fins in concert (tetraodontiform). Finally, some species spend most of their time resting on the substrate and swim only occasionally or "hop" between resting places; herein referred to as "benthic." During hops, benthic species will typically use BCF locomotion. Historically, many studies have subcategorized BCF swimming by the proportion of the body used in undulation (from anguilliform to thunniform). However, a recent study indicates that these subcategories are not kinematically meaningful (Di Santo et al., 2021).

It is important to note that all ray-finned fishes will use BCF locomotion at their maximal speeds, such as during pursuit or escape responses and will use MPF swimming to support slow swimming and fine-scale maneuvers (Blake, 2004; Sfakiotakis et al., 1999; Webb, 1984). Further, while the predominant mode of locomotion may be accomplished with a single fin, this does not preclude species from regularly using all of their fins. For example, many BCF swimmers make constant fine-scale adjustments with their MPF, thus while the caudal fin is supporting forward movement, the paired fins are stabilizing and steering the fish. Meanwhile, Labriform swimmers will use their pectorals for propulsion and maneuvers and only utilize BCF undulation at extremely high speeds or accelerations. Despite their reliance on dorsal and anal fins for propulsion, tetraodontiform swimmers will also use their pectorals frequently in steering and will employ caudal flaring and undulation to accomplish maneuvers such as backing out of tight spaces. Thus, across these main swimming categories, there is variation in functional integration in the use and cooperation of the fins. As such, shifts in patterns of fin integration with expansion into new swimming mode could be expected. However, equally plausible is that fins are always integrated because most species use all fins in some capacity to access the full spectrum of locomotion from slow maneuvers through routine swimming to high-speed modes. While functional integration alone can induce evolutionary covariation, fins are also subject to common developmental origins such as the shared epidermal fin fold of the dorsal fin, caudal fin, and anal fin (Freitas et al., 2006; Goodrich, 1906; Mabee et al., 2002; Neumann et al., 1999). Though the pectoral fin is spatially isolated from the dorsal, caudal, and anal fins, fins additionally show evidence of mutual genetic pathways that produce fin buds, fin supports, cartilage and soft tissue, and fin rays (Ahn et al., 2002; Crotwell & Mabee, 2007; Crotwell et al., 2001, 2004; Dahn et al., 2007; Heude et al., 2014; Letelier et al., 2018; Sordino et al., 1995). Thus, all fins share locomotor roles, genetic pathways, and developmental origins, which all may lead to strong evolutionary integration among fins.

Despite the many sources of potential evolutionary integration between fins, there is some evidence that independent fin evolution reflects locomotor diversity. For example, studies have explored the evolutionary integration and modularity of *fin position* relative to the body of fish, as the ability to independently adjust fin positions is considered instrumental in locomotor specialization (Drucker & Lauder, 2002; Harris, 1937; Lauder & Drucker, 2004). The two independently evolving modules of fin position that are most supported are the trunk region, which includes dorsal, anal, pectoral, and pelvic fin insertions, and the caudal region which includes the caudal peduncle and the caudal fin insertions (Aguilar-Medrano et al., 2016; Larouche et al., 2018). The positioning of fins in the trunk region was found to evolve at rates 3–5 times faster than the caudal module (Larouche et al., 2018) suggesting independent evolution of the modules. The independent evolution of the trunk module relative to the caudal module parallels the functional distinction between MPF swimming, in which the MPF is most important, and BCF swimming in which the caudal fin is most important.

In addition to fin position, fin shape is considered particularly important in the ecological filtering of reef-dwelling acanthomorph fish communities (hereafter "reef fishes"). For example, wrasses with high aspect ratio (AR) pectoral fins (wing-like and elongate) are found more often in high-exposure environments with more wave energy than species with low AR fins (paddle-like and rounded; Bellwood & Wainwright, 2001). Additionally, high AR caudal fins (deeply forked) are associated with depth-generalists, many of which swim over greater distances in depth migrations (Bridge et al., 2016). High AR fins experience less drag than low AR fins and are likely cost-efficient in conditions requiring continuous swimming. In contrast, low AR fins such as rounded caudal fins are more common on shallow reefs, presumably because higher surface area fins are beneficial in drag production needed for maneuvering in complex reef structures (Blake, 2004; Bridge et al., 2016; Lindsey, 1978; Sfakiotakis et al., 1999; Webb, 1984). These studies suggest that fin shape is functionally important to the swimming capacity of reef fishes and that changes in fin shape may have significant functional costs in swimming ability.

The combination of plausible integration among fins, independent evolution in the caudal module, and ecomorphological specialization in fins, begs the question of how morphological and functional diversity evolve within the complex locomotor system of reef fishes. Each fin may individually experience functional constraints on patterns of evolution and accumulation of diversity. However, as components in an integrated system, functional constraints on a single fin may influence the evolution of each other fin in the system. Thus, painting a complete picture of the diversification of the reef fish locomotor system requires uncovering the impact of axes of integration on functional and morphological diversification.

Reef fish lineages established associations with reef structure from 20 to 150 Mya, and began diversifying extensively following the end-Cretaceous mass extinction (Bellwood & Wainwright, 2002; Bellwood, Goatley, et al., 2014; Bellwood, Hoey et al., 2014; McCord et al., 2021; Sorenson et al., 2013; Wood, 2003). Of all clades within Actinopterygii, reef fishes span exceptional diversity in swimming mode and morphology. In this study we use reef fishes as a model system to ask, (a) Are fin shape morphospace occupation and rates of fin evolution sensitive to a fish's predominant swimming mode, (b) Are the fins of reef fishes evolutionarily integrated, and (c)

what is the effect of swimming mode on patterns of evolutionary integration among fins?

Methods

Fin morphology data collection and processing

We photographed 321 cleared and stained specimens (Dingerkus & Uhler, 1977), representing 106 species from 38 families of reef fishes, (Burns et al., In Review). We sampled 1–7 individuals with a mean of 3.02 specimens per species (Supplementary Table S1). Specimens were all of adult morphology. Generally, we did not preferentially sample a specific sex as the sex of most reef fish species is not easily identifiable without dissection. Specimens were sampled to be representative of the most abundant and speciose reef fish families (Bellwood & Wainwright, 2002), and were accessed through the aquarium trade. Our sampling covers most of the ecological diversity of reef fishes and about half of all reef fish families. For each specimen, we fully extended and pinned the pectoral, caudal, dorsal, and anal fins onto thin foam sheets permeable to light. We opted not to photograph the pelvic fin, as it is absent in some species in our data sets and is not considered an essential fin for generating thrust in any swimming category we use. Though data on the routine fin extinction used in situ was unavailable, we aimed for consistency in the tension applied to extend fins. We used photographs from the John E. Randall Fish Photo Collection at the Bishop Museum, and Google image searches as a guide for ensuring fins were not over or under-extended. We used clay block supports where needed to position the fish's body so the fin could lay flat against a level light box surface. We took images of the specimens in lateral view with a Canon digital single-lense reflex camera mounted to a level fixture such that the lens was parallel to the light box.

Shapes of the pectoral, caudal, dorsal, and anal fins were digitized in the statistical software R (version 4.2.0; R Core Team, 2022) using the package *StereoMorph* (version 1.6.7; Olsen & Westneat, 2015). As there is a great amount of diversity in the presence and number of fin spines and rays, there are few homologous landmarks on fins across our collection of reef fishes. Thus, to capture the fin shape we opted to use a sliding semi-landmark perimeter curve outlining the fin shape. We placed a single fixed landmark on the fins at the anterior-most (dorsal and anal) or dorsal-most (pectoral and caudal) insertion of the fin to anchor the perimeter curves. As for most cleared and stained specimens, the connective tissue between fin spines or rays is transparent, we placed the outlining curve along the tips of spines and rays. As such variation in soft tissue between individual spines or rays is not an aspect of fin shape variation we could capture. For species with split dorsal fins, the perimeter curve followed the dorsal edge of the body between the spines and rays. For species lacking spines in the anal and dorsal fins, the perimeter curve began and ended at the anterior insertion of the rays. To generate a matrix of coordinates representing the shape of each fin, the perimeter curves were randomly sampled 100 times where the first sample is the fixed landmark that anchors the curve (Supplementary Figure S2). For each fin type individually, fin shape coordinates were scaled and aligned using a Generalized Procrustes Analysis (GPA) in the R package *geomorph* (version 4.0.5; Adams et al., 2024; Baken et al., 2021) to remove the effects of size and rotation on fin shape variation. We then calculated species-averages of the position of each coordinate across the sampled individuals for each species. The species-average fin shapes are used in all comparative analyses (N = 106).

Categorization of swimming mode and phylogeny

Each species in our data set was categorized into swimming groupings by their predominant mode used during routine straight-path swimming (Supplementary Figure S1 and Table S1). We used four swimming categories: BCF swimming, labriform swimming, tetraodontiform swimming, and benthic fishes (Breder, 1926; Fulton, 2007; Korsmeyer et al., 2002; Lindsey, 1978; Webb, 1984). Labriform swimming is named after Labridae which is the most exemplar clade of pectoral fin swimming, though many reef fishes outside of Labridae also use labriform swimming. However, a single clade in our species set, the Tetraodontiformes, uses tetraodontiform swimming. Benthic species are periodic swimmers that spend most of their time resting in direct contact with the substrate.

In preparation for phylogenetic analyses, we created a phylogeny of the 106 species in our data set using the R package *FishTree* (version 0.3.4) to trim a large (11,638 species) time-calibrated phylogeny of ray-finned fishes estimated using 27 mitochondrial and nuclear coding genes (Chang et al., 2019; Rabosky et al., 2018). In cases where species in our dataset were not present in the larger phylogeny, we used the most closely related species present in the larger phylogeny as a substitution (Supplementary Table S1). We used an ancestral state reconstruction to map the history of swimming mode transitions onto the phylogeny (Figure 1; Supplementary Figure S3) using *phytools* (version 1.9.16; Revell, 2024) and *ape* (version 5.7.1; Paradis & Schliep, 2019). Specifically, we generated 100 stochastic character maps, with the highest likelihood estimated transition matrix (Q), and calculated swimming mode transition probabilities at nodes.

Analyses of fin shape and swimming mode

All analyses were performed in R (version 4.2.0; R Core Team, 2022). We generated fin shape morphospaces (Figure 2; Supplementary Figures S4–S6) using a Principal Component Analysis (PCA) on the variance-covariance matrix of fin shape coordinates using the *gm.prcomp* function in the package *geomorph* (version 4.0.7; Adams et al., 2024; Baken et al., 2021). Reference shapes for the morphospaces (grey fins in the background of Figure 2; Supplementary Figures S5 and S6) were generated using the *btShapes* function in *Stereomorph*. We chose to display morphospaces as ordinary PCAs rather than phylogenetically corrected PCAs as these visuals mirror the occupation of fin shape space on coral reefs, allowing for a straightforward interpretation of morphological variation. While some families in our samples are more heavily represented than others, this reflects the prominence of more abundant and speciose families on reefs.

For each fin, we used *geomorph* and *RRPP* (version 2.0.0; Adams et al., 2024; Collyer & Adams, 2018, 2024) to test for differences in mean fin shape using the GPA-aligned coordinates between swimming groups with phylogenetic analysis of variance (ANOVAs) (*procD.pgls, 1000 iterations for permutations*) and post-hoc comparisons (*pairwise*, Table 1), and to estimate shape disparity within each swimming group (*morphol.disparity*, *10,000 iterations for permutations*; Supplementary Table S2).

We further explored regions of fin morphospace uniquely occupied by a single swimming group and the degree of

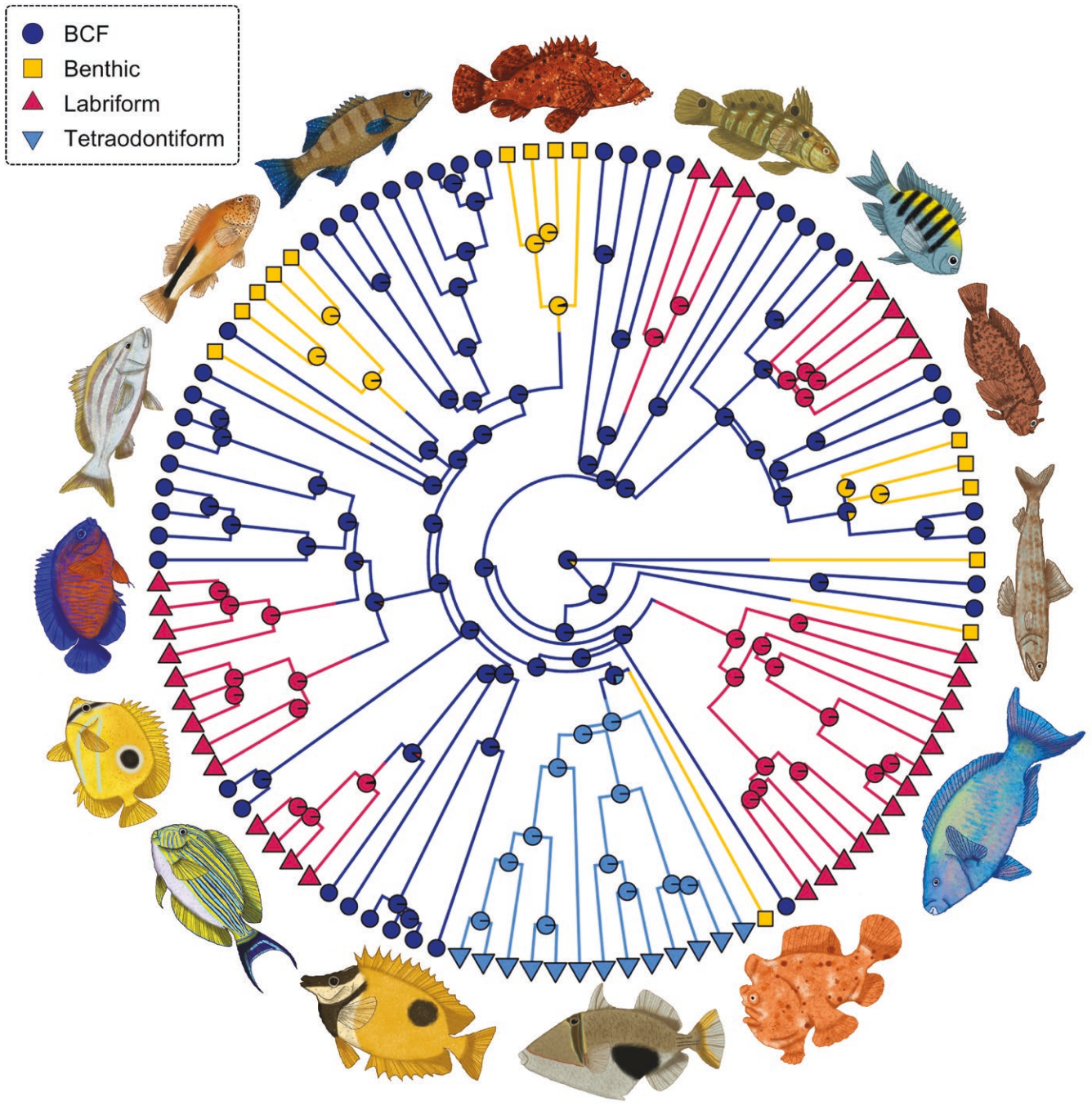

Figure 1. Stochastic character map of the history of swimming mode, with pie charts indicating the node state percentage out of 100 maps. Dark blue circles represent body-caudal fin swimmers, which use the undulation of their body and caudal fin to move forward. Magenta triangles represent lineages that use pectoral fins as the predominant propulsor (labriform), and light blue inverted triangles represent lineages that use the dorsal and anal fin for propulsion (tetraodontiform). Yellow squares represent benthic species.

morphospace overlap between swimming groups using fin shape hypervolumes generated in the R package *hypervolume* (version 3.1.3; Blonder et al., 2023). While our ANOVAs allowed us to assess whether mean fin shape varies by swimming mode, hypervolume analyses allowed us to construct multidimensional morphospace volumes for groups of species within a swimming group and outside of a swimming group. Here we had a total of eight hypervolumes: BCF, Labriform, Tetraodontiform, Benthic, Non-BCF, Non-Labriform, Non-Tetraodontiform, and Non-Benthic. We compared hypervolumes, for example, the BCF species versus all non-BCF species, to determine what volume of morphospace is shared, and what fraction of each volume is unique morphospace (Figure 3A; Table 2 and Supplementary Table S3). To test the significance of our estimates of unique volume, we generated a null distribution of the fraction of volume unique to one hypervolume by permuting species between hypervolume assignments, such that species are randomly redistributed between the two hypervolume assignments in comparison (Figure 3A). We iterated this permutation procedure 10,000 times, and for each iteration, we recorded the fraction of morphospace volume that is unique to each permuted hypervolume (Figure 3B).

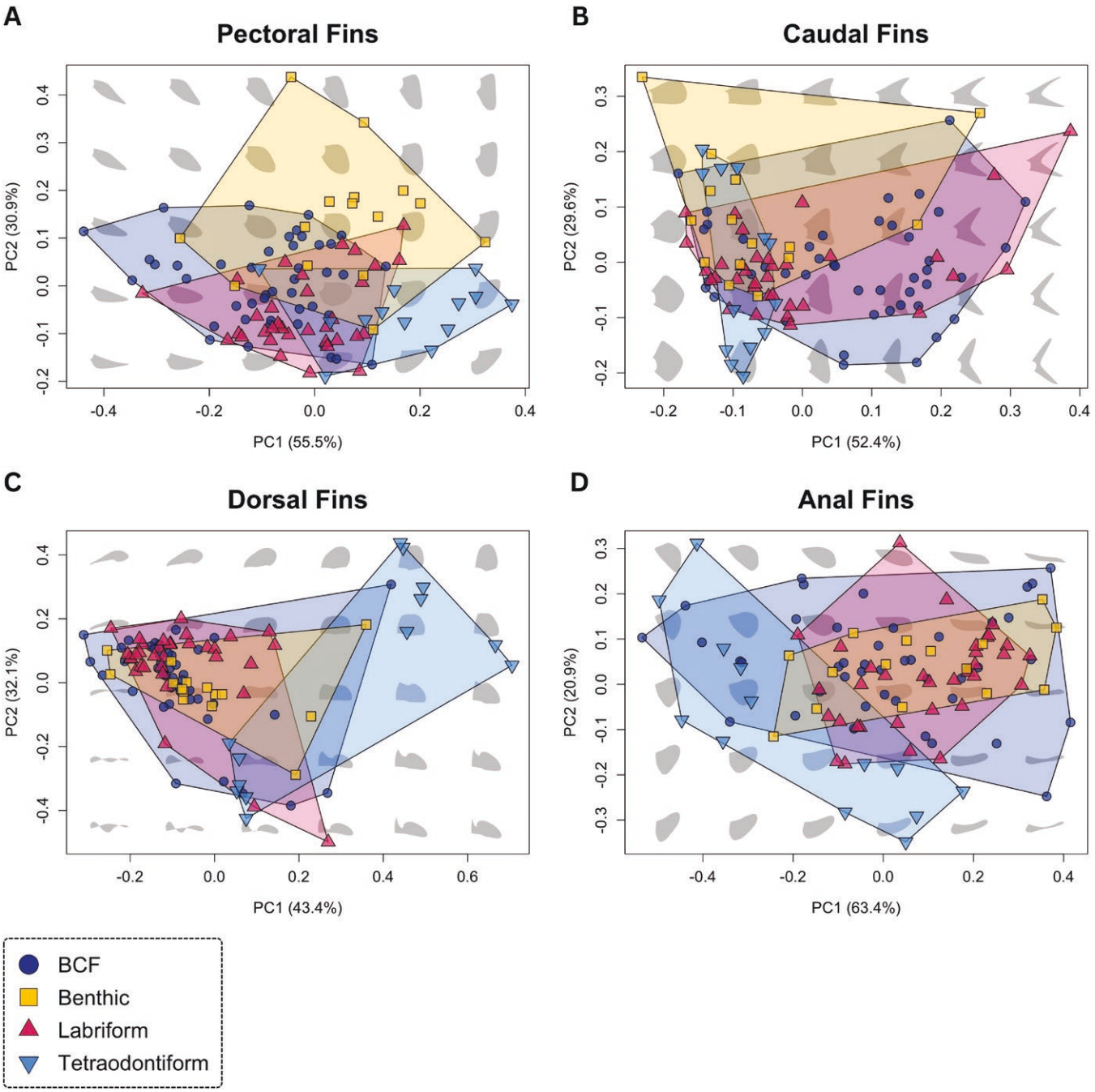

Figure 2. Fin shape diversity by swimming mode. (A) Fin shape morphospaces for the pectoral fin, (B) caudal fin, (C) dorsal fin, and (D) anal fin. Each point represents the average Procrustes superimposed fin shape for a species. Dark blue circles represent body-caudal fin swimming species. Yellow squares are benthic species. Magenta triangles represent labriform swimming species. Light blue inverted triangles are tetraodontiform swimming species. Swimming modes are highly overlapping in morphospace. Notable exceptions are that benthic species have pectoral fins with greater ventral ray elongation, and labriform swimmers have greater dorsal ray elongation. The tetraodontiform swimmers have shorter and deeper dorsal and anal fins on average. $N = 106$.

The distribution of the fraction of unique volume from the permuted hypervolumes represents a null distribution. We compared our true unique fractions to the distributions of permuted values. We calculated a p-value as the proportion of the permuted distribution greater than the true value. A hypervolume was found to be more unique than expected (a higher volume of non-overlap) if the true unique volume fell beyond the upper 2.5% tail cut-off of the null distribution ($p < 0.025$). A hypervolume was less unique than expected (a lower volume of non-overlap) if the true unique volume fell beyond the lower 2.5% tail cut-off of the null distribution ($p > 0.975$; Figure 3B). There were three types of possible significant outcomes of these hypervolume analyses, (a) Both hypervolumes in comparison are non-overlapping and significantly unique from one another, (b) hypervolume X occupies a volume of morphospace that is significantly unique from Y, but most of Y's volume is contained within X, and (c) both hypervolumes overlap significantly with each other (Figure

Table 1. Mean fin shape by swimming mode ANOVAs.

	Pectoral	Caudal	Dorsal	Anal
Phylo. ANOVA				
p	**0.003**	0.105	**0.007**	0.216
F	**3.455**	1.756	**2.658**	1.416
Pairwise comparison				
BCF: Benthic	**0.011**		0.627	
BCF: MPF—Lab.	0.642		0.900	
BCF: MPF—Tet.	0.302		**0.043**	
Benthic: MPF—Lab.	0.202		0.822	
Benthic: MPF—Tet.	0.525		0.134	
MPF—Lab.: MPF—Tet.	0.466		**0.036**	

Note. *p* values and *F* statistics where the mean fin shape significantly differs by locomotor mode are bolded. For fins with different mean fin shapes by locomotor mode, the pairwise least squares comparisons are provided to indicate which locomotor groups differ in shape from each other.
BCF = body-caudal fin; MPF = median and paired fin.

3C). Note that type 2 can be reversed such that Y can be unique from X, but the volume of Y contains the volume of X.

We ran two types of hypervolume comparisons for each fin: (a) A focal swimming group against all other species (e.g., BCF swimmers vs. all non-BCF swimmers), (b) pairwise swimming group comparisons (e.g., BCF swimmers vs. Labriform swimmers; Figure 3D). This process produced a total of 10 hypervolume comparisons for each fin: four focal swimming group comparisons, and six pairwise comparisons. The data we used to construct the hypervolumes were the principal component (PC) axes of fin shape as the raw fin coordinates are too multidimensional to include. To determine the number of PC axes for each fin shape that explained a great enough proportion of overall shape variance to warrant inclusion in the hypervolume construction, we used a broken-stick method (MacArthur, 1957). Under this method, a PC is retained if the proportion of variance it accounts for is greater than the total variance divided by the total number of components (100 in our case: 1 fixed landmark, and 99 curve points). This method determined that five PCs were sufficient to include the pectoral and anal fins. However, the dorsal fin and caudal fin require six PCs. We provide a visual example of the hypervolume analyses using the pectoral fin focal versus non-focal group comparisons in Figure 4.

We evaluated the evolutionary correlation between fins with calculations of phylogenetic integration and rates of fin shape evolution in *geomorph*. To determine if the evolution of novel swimming modes co-occurs with reductions in fin integration, we estimated integration first for all species, and secondly within each swimming mode (Table 3; Figures 5 and 6). To visualize the fin shapes that commonly occur together, we plotted the fin-by-fin comparisons from non-phylogenetic two-block partial least squares (PLS) regressions (Figure 6). This is helpful as plotting the PLS axes of the fins from the phylogenetic integration tests would instead show relationships between residual variation in fin shape once the phylogeny is accounted for and thus does not easily translate to the original fin shapes. In summary, we used non-phylogenetic PLS axes for visualization, but statistical interpretations of the evolutionary integration are taken from phylogenetically corrected analyses (*phylo.integration, 1000 iterations*).

Figure 5 shows the effect size of integration by swimming group for each pairwise fin integration test. Effect size here is a measure of the strength of the signal of phylogenetic integration accounting for sample sizes. As such, effect sizes are useful in comparing integration strengths across systems and studies. Here, we use effect size to compare the strength of integration across groups with unequal numbers of species. The *phylo.integration* function in *geomorph* calculates the effect size of the integration statistic, *R*, as a *z*-score, or a standard deviate of a null distribution of *R* values calculated for resampled permutations (see Adams & Collyer, 2019). As such, a larger effect size (*Z*) indicates the true *R*-value is further away from the mean of the null distribution. Integration is significant when the true *R*-value is greater than 95% of values in the null distribution (a value of $Z = 2$ for a perfectly normal distribution). In the present case, a significant *Z* may be detected at a value less than 2 if the null distribution is slightly skewed to the right.

To compare overall rates of evolution between the fins for all species, we combined the independently GPA-aligned coordinates for each fin type using the "*combine.subsets*" function with centroid sizes provided for scaling. Prior to estimating evolutionary rates, we compared the fit of single-rate Brownian motion (BM), multi-rate Brownian motion (BMS), single-rate/single optimum OU (OU1), single-rate/multi-optima OU (OUM), and multi-rate/multi-optima OU (OUVM) models of evolution on the fin ARs (fin length^2/surface area) using the "*OUwie*" function in the R package *OUwie* with 1,000 iterations (Beaulieu et al., 2012; O'Meara et al., 2006). For each fin, BMS was the most likely model (Supplementary Table S4). Therefore, we used "*compare.multi.evol.rate*" to estimate the multivariate Brownian rates for each set of fin landmarks with 1,000 iterations to test for significance. To assess the effects of swimming mode on Brownian rates of fin shape evolution, we estimated the rates among species within a swimming group for each fin using the function "*compare.evol.rate*" in *geomorph* (Figure 7), again with 1,000 iterations.

Results

Evolutionary history of swimming mode

Of the 106 species in our fin data set, we categorized 44 as BCF, 15 as benthic, 34 as labriform, and 13 as tetraodontiform. The average number of transitions between swimming

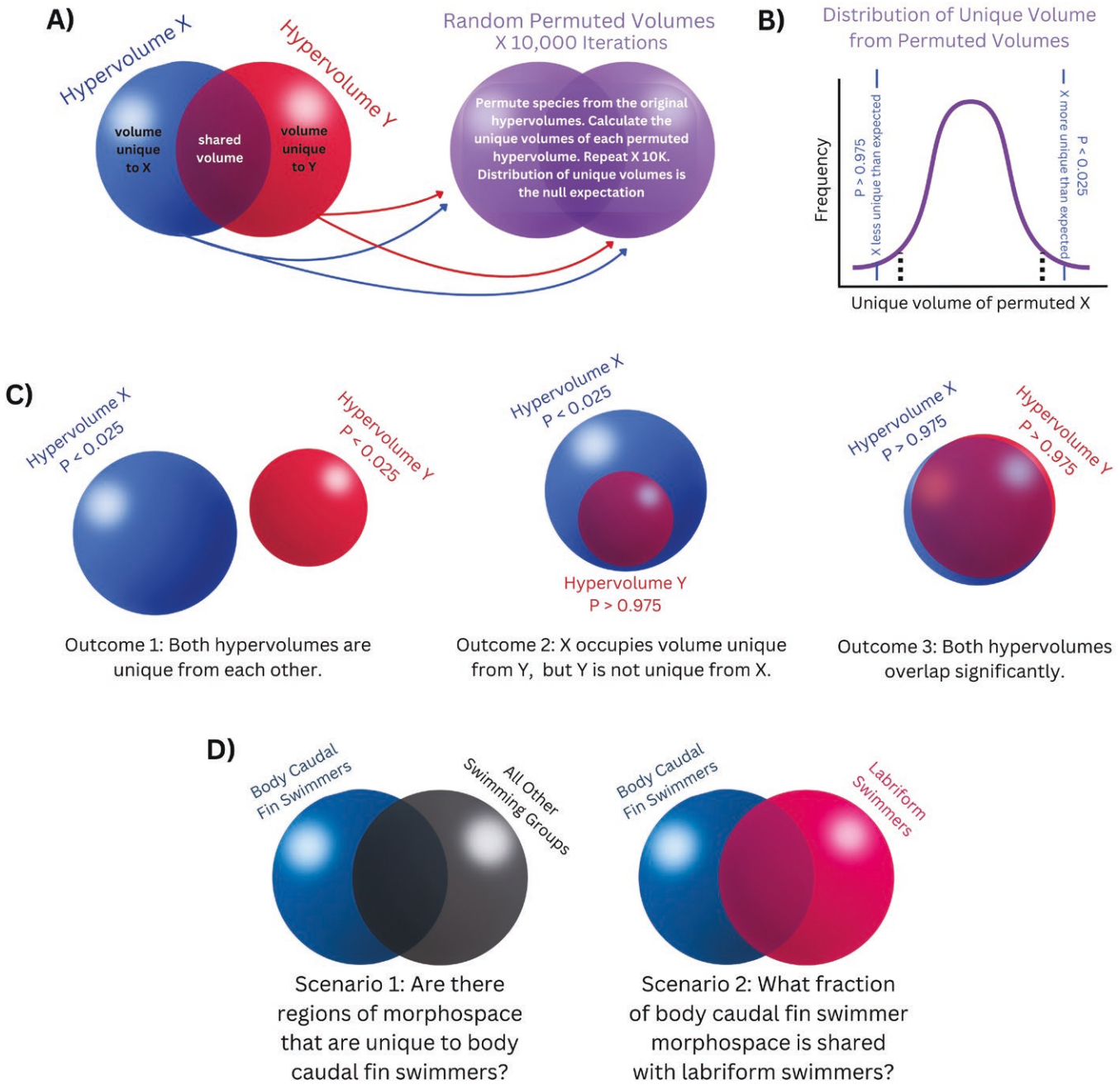

Figure 3. Hypervolume method used to estimate unique fin morphospace occupation. (A) Hypervolumes are generated from the positions of species in multidimensional morphospace. We can compare two hypervolumes and calculate the volume of morphospace that is non-overlapping or unique. We then randomly permute the hypervolume assignments for each species, estimate new hypervolumes on the permuted data, and calculate the unique volumes. Repeating the permutations and calculations 10,000 times provides (B) a null distribution for a volume of interest, such as the unique volume of permuted hypervolume X. We can compare the position of the true value for the volume of morphospace unique to hypervolume X to the distribution of permuted values. If the true value is in the lower tail ($p > 0.975$), hypervolume X occupies less unique morphospace than expected at random. If the true value is in the upper tail ($p < 0.025$), hypervolume X occupies more unique morphospace than expected at random. (C) There are three possible significant outcomes of hypervolume analyses: (1) X and Y occupy unique volume from each other, (2) X has a volume unique from Y, but Y is not unique from X, and (3) X and Y overlap significantly. (D) In this study we perform two types of hypervolume analyses. The first asks whether species in one swimming mode occupy a volume of morphospace that is unique from all other species. The second compares swimming modes in a pairwise manner, asking if two modes occupy volumes of morphospace that are unique from one another or overlap significantly.

modes from 100 stochastic character maps (simmaps) was 17.26 transitions. The most common ancestral state was BCF in 86.6% of the simmaps, followed by benthic at 10.5% of the simulations, and only 1.4% for both labriform and tetraodontiform. The most common transition was from BCF to benthic with an average of 7.99 transitions, followed by 6.25 transitions from BCF to labriform, 1.35 from benthic to BCF, and finally 1.01 from BCF to tetraodontiform (Figure 1, Supplementary Figure S3). The simmaps recovered no other transitions between modes, for example, there were no transitions from labriform swimming back to BCF swimming.

Effects of swimming mode on fin shape diversity in reef fishes

The fin-shape morphospaces we have constructed represent the first comparative dataset of fin-shape diversity across reef

Table 2. Hypervolume results.

Hv1	Hv2	Observed unique frac. Hv1	*p*-value Hv1	Observed unique frac. Hv2	*p*-value Hv2
Pectoral					
BCF	Not BCF	0.215	0.8176	0.668	**0.0149**
Benthic	Not Benthic	0.860	**0.0001**	0.273	0.8662
Labriform	Not Labriform	0.110	**0.9772**	0.824	**0.0004**
Tetraodontiform	Not Tetraodontiform	0.397	0.2603	0.871	**0.0152**
Caudal					
BCF	Not BCF	0.537	0.1971	0.473	0.3536
Benthic	Not Benthic	0.239	0.6944	0.861	0.0416
Labriform	Not Labriform	0.325	0.5258	0.632	0.1695
Tetraodontiform	Not Tetraodontiform	0.494	0.2305	0.919	**0.0147**
Dorsal					
BCF	Not BCF	0.342	0.6369	0.748	0.0819
Benthic	Not Benthic	0.358	0.5247	0.796	0.2182
Labriform	Not Labriform	0.237	0.8298	0.850	0.0298
Tetraodontiform	Not Tetraodontiform	0.960	**0.0000**	0.773	0.2806
Anal					
BCF	Not BCF	0.596	**0.0157**	0.304	0.5364
Benthic	Not Benthic	0.337	0.3548	0.623	0.2030
Labriform	Not Labriform	0.053	**0.9981**	0.889	**0.0000**
Tetraodontiform	Not Tetraodontiform	0.674	**0.0134**	0.802	0.0310

Note. Comparisons of the hypervolumes of species within a locomotor group against the hypervolume of all other species. Light-shaded columns are data for the first hypervolume, and dark-shaded columns are for the second hypervolume in the comparison. Column titles with "Observed unique fac." are the observed fraction of volume unique to the hypervolume. Column titles with "*p*-value" are the proportion of the 10,000 permuted hypervolumes which have a fraction of the unique volume that is greater than the observed value. As such, if the *p*-value is 0.975, 97.5% of permutations yielded a larger uniqueness than the observed value. In contrast, if the *p*-value is 0.025 only 2.5% of permutations yielded a greater uniqueness. Significant *p* values beyond these cut-offs are bolded. Real hypervolumes and random permutations were generated in *Hypervolume (v 3.1.3; R)*.
BCF = body-caudal fin.

fishes (Figure 2; Supplementary Figures S4–S6). The first axis of pectoral fin diversity (PC1) separates fins by what is commonly referred to as AR, or an axis of narrow, wing-like fin shapes (e.g., *Caranx ruber*) to deep, paddle-like fin shapes (e.g., *Diodon holocanthus*, Figure 2A; Supplementary Figure S4). The elongation of the pectoral fin at the lower half of PC1 is possible through a lengthening of the leading edge, trailing edge, or central rays of the fin. This variation in which parts of the fin are lengthened falls out on the second axis of pectoral fin variation, reflecting the ratio between the length of the leading and trailing edges of the fin. Here, species that score high on PC2 have longer trailing edges of the fin (e.g., *Cirhitichys falco*) and species with low PC2 scores have longer leading edges (e.g., *Acanthostracion quadricornis*, Figure 2A, Supplementary Figure S4). We detect a significant effect of swimming mode on mean pectoral fin shape (Table 1; $p = 0.003$, $F = 3.455$, $df = 3,105$). Specifically, the mean BCF pectoral shape is more wing-like (low PC1) than other swimming groups. Only benthic species occupy the region of morphospace with elongated trailing edges (high PC2, Figure 2A, Supplementary Figure S4). Labriform and tetraodontiform swimmers occupy the mid to upper region of PC1 and lower region of PC2, with generally more paddle-like fins where the leading edge is more elongate. Labriform swimmers are more central in pectoral fin shape than tetraodontiform swimmers (Figure 2A, Supplementary Figure S4). We note, however, that in pairwise comparisons BCF versus benthic species are the only pair with statistically different mean pectoral shapes ($p = 0.001$).

The first two axes of caudal fin shape diversity separate fins that are (a) rounded (low PC1) to forked (high PC1) and (b) deep (low PC2) to narrow (high PC2). The most rounded caudal fin shape is in *Plesiops coeruleolineatus* and the most forked caudal belongs to *Genicanthus melanospilos* (Figure 2B, Supplementary Figure S4). The swimming groups highly overlap in the caudal fin morphospace, showing no differences in mean fin shape (Table 1; $p = 0.105$, $F = 1.756$, $df = 3,105$). BCF, benthic, and labriform swimmers occupy a wide array of shapes, spanning both PC1 and PC2. However, the tetraodontiform caudal occupies a narrower region of PC1 in which the caudal fins are slightly more rounded than square (e.g., *Stephanolepis hispidus*), though the mean shape is not significantly different from the mean of the other swimming groups (Figure 2B, Supplementary Figure S4). It should be noted that of the 34 labriform species and 15 benthic species, only six labriform (three pomacentrids, two acanthurids, and a pomacanthid), and two benthic species (*Ecsenius midas* and *Synodus saurus*) have heavily forked caudal fins (Figure 2B, Supplementary Figure S4). Most of the labriform swimmers with forked caudals are more planktivorous and occupy the midwater column more frequently than their close relatives. Both benthic species with forked caudals are more elongate in body shape than other benthic species. In contrast, BCF swimmers more evenly occupy the array of caudal fin shapes and there are not obvious ecological associations that distinguish BCF swimmers with rounded or forked caudal fins, though future studies with data on ecology may detect patterns.

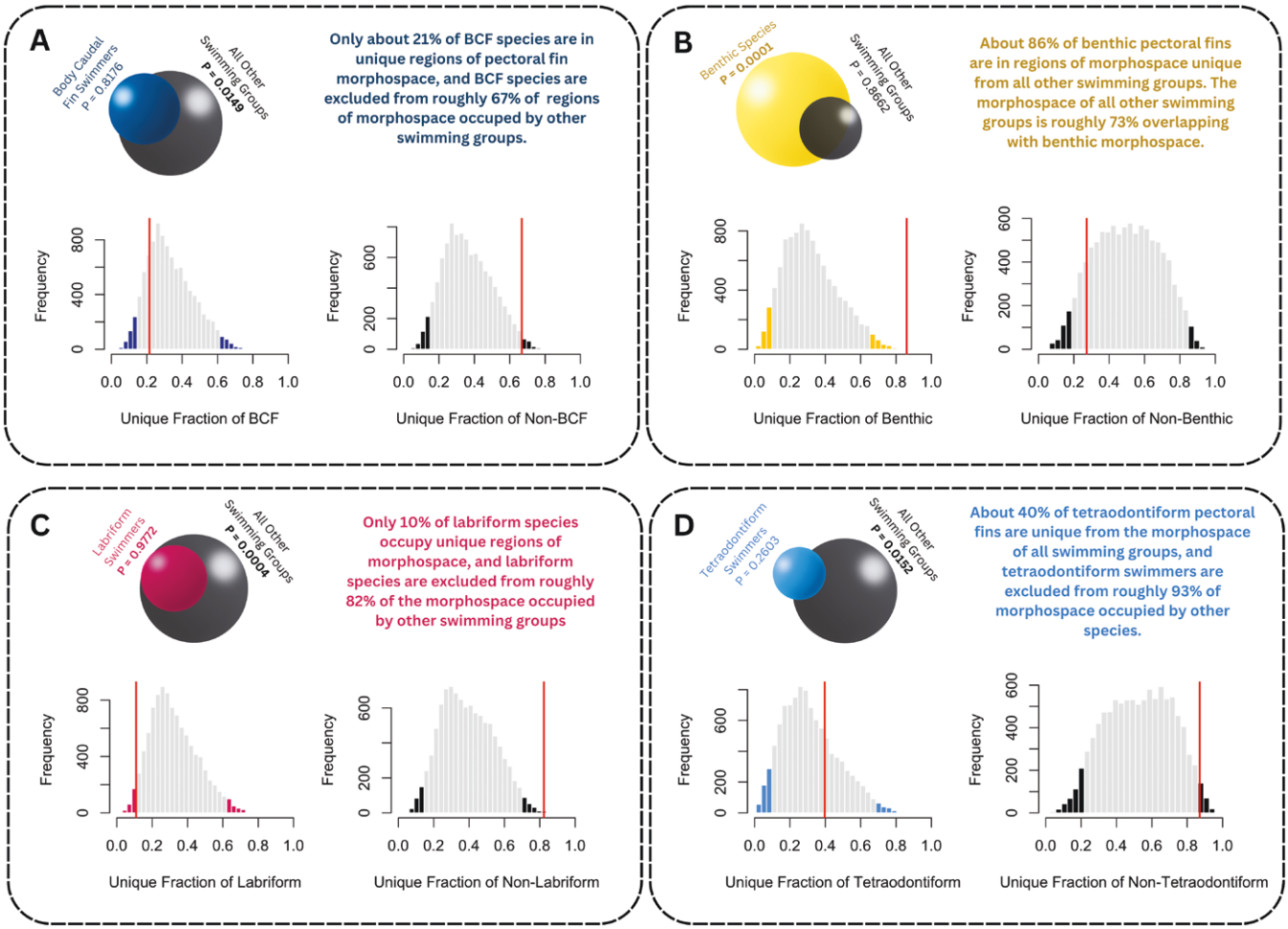

Figure 4. Pectoral fin hypervolume comparisons. The results shown here are the comparisons between a focal swimming group versus all other species. For example, (A) body-caudal fin species versus all other species. Each panel contains an illustration (spheres) that represents the relationship between the two volumes in comparison. The panels also show the distribution of permuted unique fractions for each hypervolume. *p* values indicate the number of permutations for which the unique fraction was greater than the observed value. Shaded tail regions indicate the upper and lower 2.5% of the distribution. Red vertical lines indicate the observed unique fraction of the hypervolume. (B) Benthic species versus all other species. (C) Labriform species versus all other species. (D) Tetraodontiform species versus all other species. Key results are described in the text in the panels.

The dorsal fin morphospace is the most intricate, and the primary axes of diversity are the most complex. PC1 represents both the gradient in dorsal fins that are elongate and low-lying (e.g., *Hoplolatilus fronticinctus*, low PC1) to those that are short and deep (e.g., *Canthigaster solandri*, high PC1), and dorsal fins with longer posterior rays (low PC1) relative to longer anterior spines (Figure 2C, Supplementary Figure S4; high PC1). PC2 separates fins that have a significant separation between the spiny and soft dorsal (e.g., *Cantherhines pullus*; low PC2) and continuous fins (e.g., *Ctenochaetus strigosus*; high PC2). Most species lay in the low PC1, mid-PC2 region of elongate continuous dorsal fins, with a subtle dip where the spines and rays meet (e.g., *Haemulon flavolineatum*). Many of the swimming groups have a large degree of overlap in the dorsal fin morphospace (Figure 2C, Supplementary Figure S4). However, we do detect a significant effect of the swimming group on the mean dorsal shape (Table 1; $p = 0.007$, $F = 2.658$, $df = 3,105$). Namely, the tetraodontiform swimmers have a mean dorsal shape significantly shorter and deeper (high PC1) than other swimming groups. However, they span the range of a single continuous dorsal (Tetraodontidae) to a split between the spiny dorsal and soft ray dorsal (Balistidae and Monacanthidae).

Like the dorsal fin, the first axis of diversity in the anal fin (Figure 2D, Supplementary Figure S4) distinguishes species that have short, deep anal fins (e.g., *Sphaeramia orbicularis*; low PC1) and those that have elongate, low-lying anal fins (e.g., *Parapercis millepunctata*; high PC1). PC2 represents a ratio of the length of the anterior-most spines (or rays in the absence of spines) of the fin to the length of the rays at the posterior of the fin, separating species with longer anterior length (e.g., *Stephanolepis hispidus;* low PC2) to longer posterior length (e.g., *Genicanthus melanospilos;* high PC2; Figure 2D, Supplementary Figure S4). Swimming groups are not distinct in mean anal fin shape (Table 1; $p = 0.216$, $F = 1.416$, $df = 3,105$). However, tetraodontiform swimmers do not occupy the high PC1 region. Labriform swimmers have anal fin shapes nested within the diversity of the other swimming modes and are more central in the morphospace. Benthic species span most of PC1 but occupy only a narrow region of PC2 where the anterior and posterior spine/ray lengths are uniform.

Swimming groups vary in the range of morphospace volume they occupy (Supplementary Table S2). For example, in the pectoral fin, benthic species have greater disparity ($D = 0.050$) than labriform swimmers ($D = 0.021$,

Table 3. Fin-by-fin comparisons of phylogenetic integration.

Fin-by-fin Phylo. Integration	All species included			Body-caudal fin			Labriform			Tetraodontiform			Benthic		
	r-PLS	Effect (*Z*)	*p*	*r*-PLS	Effect (*Z*)	*p*	*r*-PLS	Effect (*Z*)	*p*	*r*-PLS	Effect (*Z*)	*p*	*r*-PLS	Effect (*Z*)	*p*
Pectoral—Dorsal	0.30	1.24	0.116	0.46	1.08	0.149	0.60	1.77	0.050	0.49	−0.14	0.557	0.74	1.69	0.050
Pectoral—Caudal	0.39	2.87	**0.001**	0.45	1.67	**0.047**	0.41	0.98	0.182	0.44	−0.02	0.505	0.70	1.45	0.080
Pectoral—Anal	0.32	1.95	**0.023**	0.50	2.32	**0.008**	0.38	0.27	0.405	0.60	0.86	0.208	0.53	0.33	0.371
Dorsal—Caudal	0.37	2.26	**0.011**	0.54	2.07	**0.018**	0.49	1.18	0.135	0.71	1.54	0.067	0.61	0.34	0.394
Dorsal—Anal	0.61	4.90	**0.001**	0.70	3.76	**0.001**	0.65	2.25	**0.012**	0.90	2.68	**0.003**	0.76	2.17	**0.015**
Caudal—Anal	0.49	3.75	**0.001**	0.52	2.28	**0.010**	0.54	1.98	**0.024**	0.68	1.50	0.074	0.53	0.32	0.387

Note. Results were generated using *Geomorph (v 4.0.5; R)*. Statistically significant integrations were determined based on 1,000 iterations and are denoted by *p* values (*p*) which are bolded. Columns are shaded in colors to match the swimming group colors used in the figures.
PLS = partial least squares.

$p = 0.002$, $df = 1,105$) and BCF swimmers ($D = 0.029$, $p = 0.016$, $df = 1,105$). Caudal fin disparity is roughly equal for all swimming groups ($D = 0.032–0.036$, $p = 0.762–0.995$, $df = 1,105$). Interestingly, dorsal fin disparity is similar for BCF, benthic, and labriform swimmers ($D = 0.062–0.068$, $p = 0.774–0.973$, $df = 1,105$); however, tetraodontiform dorsal fins display 3× the disparity of the other swimming groups ($D = 0.197$, $p < 0.001$ for all tetraodontiform dorsal comparisons, $df = 1,105$), making the tetraodontiform dorsal the most diverse of any fin shape (Figure 4; Supplementary Table S2). Tetraodontiform swimmers also occupy the most diverse morphospace in the anal fin ($D = 0.096$), but BCF and benthic species are also high in disparity ($D = 0.080$ and 0.059, respectively, $p = 0.105–0.392$; $df = 1,105$). The labriform anal fin is less diverse than BCF and Tetraodontiform anal fins ($D = 0.042$, $p = 0.005$ in both cases, $df = 1,105$).

Effects of swimming mode on unique fin morphospace occupation

While the analyses in the previous section allow us to address the impacts of swimming mode on the mean fin shape, hypervolumes demonstrate whether the diversity of fins within swimming groups occurs within unique or shared regions of morphospace (Figures 3 and 4; Table 2 and Supplementary Table S3). Though we use spheres as illustrative symbols, true hypervolumes account for large gaps in morphospace, such that these highly dimensional volumes can have "donut-holes" where no species are present. This contrasts the two-dimensional morphospaces shown in Figure 2 and Supplementary Figures S5 and S6 where convex hulls surround the most outlying species. The range of significant results observed when comparing the unique morphospace occupation of a focal swimming group to all species not in that swimming group (non-focal group species) were that (a) the focal group is significantly unique and non-overlapping with all other species, (b) the focal group is not unique and largely contained within the volume of all other species, (c) the focal group is significantly unique and the focal group volume contains the volume of all other species, and (d) the focal group and all other species overlap greatly and neither volume is unique. Figure 4 shows the results of focal group comparisons for the pectoral fin, illustrating how the observed fraction of unique volume of the focal group and non-focal group hypervolumes, and the associated *p* values can be used to understand the overlap between the morphospace volume occupied by the two groups. Table 2 provides the results for all focal group to non-focal group comparisons for all fins. Focal group to focal group (e.g., BCF vs. Labriform) comparisons can be found in Supplementary Table S3.

We find that for the pectoral fin, roughly 80% of the volume of BCF species overlaps with the volume of other species, and therefore BCF species are not significantly unique. However, BCF species only occupy 33% of the volume of other species. In other words, BCF species are excluded from 67% of the volume of all other species (Figure 4A). In contrast, the volume of morphospace that benthic species occupy contains 73% of the volume of all other species, and 86% of the benthic volume is unique ($p = 0.0001$, $df = 1,105$; Figure 4B). Labriform species are 89% contained within the volume of other species, and therefore significantly less unique than expected under a null model ($p = 0.9772$, $df = 1,105$; Figure 4C). Labriform species are also significantly excluded from 82% of the morphospace volume of all other species

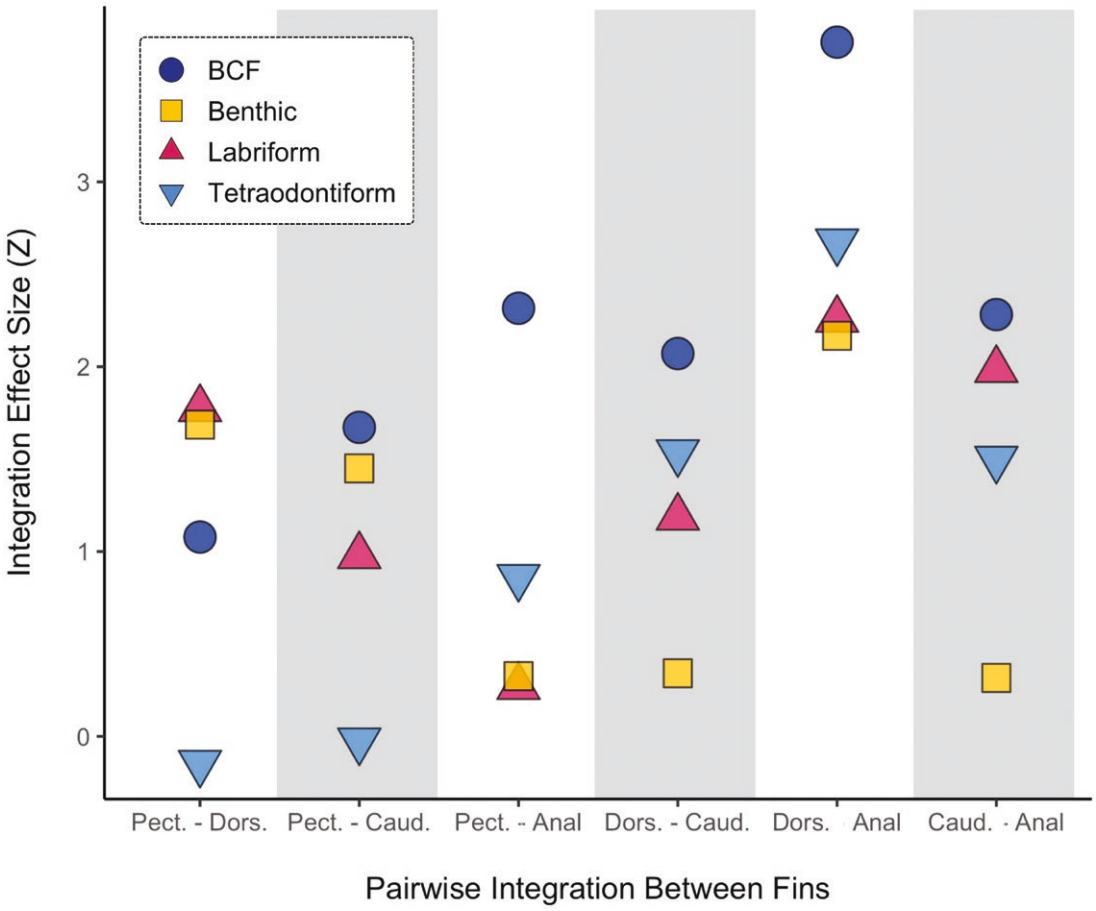

Figure 5. Phylogenetic integration effect sizes by swimming mode. Along the *x*-axis pairwise fin combinations are separated by the shaded vertical bands. The *y*-axis is the effect size (*Z*) coefficient from the phylogenetic integration tests. Dark blue circles represent integration among body-caudal fin (BCF) swimming species. Yellow squares represent integration among benthic species. Magenta triangles represent integration among labriform swimming species, and light blue inverted triangles represent integration among tetraodontiform swimming species. Note that for 5 out of 6 fin combinations, the effect size (the strength) of the integration for BCF swimmers is greater than or equal to the effect size for derived swimming modes.

(p = 0.0004, df = 1,105; Figure 4C). About 40% of the tetraodontiform pectoral fin volume is contained within the volume of all other species, thus tetraodontiform swimmers are not significantly unique or unexpectedly overlapping with other species (p = 0.2603, df = 1,105; Figure 4D). However, tetraodontiform swimmers are excluded from 93% of the volume of pectoral fin morphospace occupied by other species (p = 0.0152, df = 1,105; Figure 4D).

We find one significant result for the caudal fin: tetraodontiform swimmers are significantly excluded from 92% of the non-tetraodontiform morphospace (p = 0.0147, df = 1,105). In the dorsal fin, tetraodontiform swimmers occupy 96% unique morphospace (p < 0.0001, df = 1,105). Though just short of the cut-off for significance, the labriform dorsal fin is excluded from 82% of the dorsal morphospace volume for all other species (p = 0.0297, df = 1,105). Finally, for the anal fin, 60% of the BCF morphospace volume is unique (p = 0.0157, df = 1,105), but the BCF volume is not excluded from regions of morphospace occupied by other species (p = 0.5364, df = 1,105). Labriform species occupy less unique anal fin morphospace than expected under a null model (only 5.3% unique, p = 0.9981, df = 1,105) and are excluded from 89% of the anal fin morphospace volume that non-labriform swimmers occupy (p < 0.0001, df = 1,105). Additionally, 68% of the tetraodontiform anal fin morphospace volume is unique (p = 0.0134, df = 1,105), and tetraodontiform swimmers are excluded from 80% of the morphospace volume of all other species (though this result is not significantly beyond null expectations, p = 0.0310, df = 1,105).

The possible outcomes of pairwise hypervolume comparisons between swimming groups were that (a) one swimming group occupied a significantly unique morphospace, but contained the volume of the other group, (b) both swimming groups were largely non-overlapping and significantly unique from one another, and (c) both swimming groups were highly overlapping and neither was significantly unique in morphospace occupation (see Supplementary Table S3 for proportions of the hypervolumes that were unique in morphospace and the associated p values).

For the pectoral fin, the benthic species hypervolume overlapped little with BCF, labriform, and tetraodontiform swimmers (between 88% and 99% unique, see Supplementary Table S3 for statistics). Additionally, the BCF pectoral hypervolume was 82% unique from tetraodontiform swimmers (p = 0.0136, df = 1,105). Although, tetraodontiform swimmers are 40% contained within (and thus not significantly unique from) BCF swimmers (p = 0.0916, df = 1,105). The labriform occupation of the pectoral fin morphospace was never statistically unique, indicating labriform swimmers had a large volume nested within the BCF, benthic, and tetraodontiform

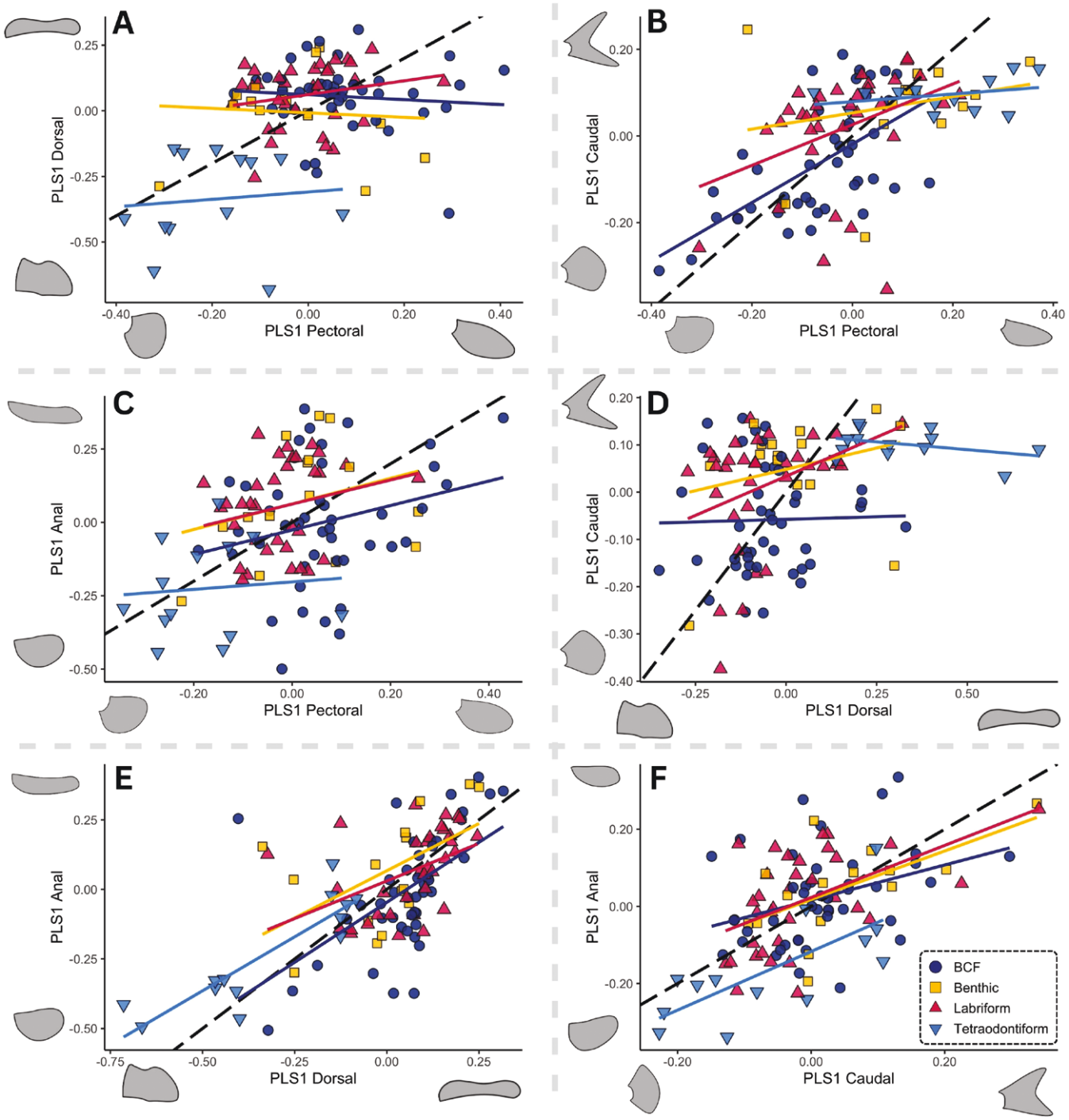

Figure 6. First partial least squares regressions depicting morphological correlation between fin shapes. Linear relationships showing non-phylogenetically corrected morphological integration between fins: (A) dorsal vs. pectoral, (B) caudal vs. pectoral, (C) anal vs. pectoral, (D) caudal vs. dorsal, (E) anal vs. dorsal, (F) anal vs. caudal. Each point represents the first partial least squares score for a species. Dark blue circles represent body-caudal fin swimming species. Yellow squares are benthic species. Magenta triangles represent labriform swimming species. Light blue inverted triangles are tetraodontiform swimming species. The dashed black line is the overall integration trendline for all species. The trendline for integration within each locomotor group is also displayed as a solid line matching the color of the points. $N = 106$.

hypervolumes. For the caudal fin, the BCF hypervolume was 93% unique relative to tetraodontiform swimmers, and 86% unique from Benthic species (Supplementary Table S3). Tetraodontiform swimmers shared little dorsal fin morphospace with any of the other three swimming groups, ranging from 95% to 98% unique (Supplementary Table S3). Finally, for the anal fin, the BCF morphospace volume contains 89% of the labriform volume but is itself 87% unique from the morphospace labriform swimmers occupy. BCF and tetraodontiform swimmers are both highly unique from one another in anal fin morphospace, as are benthic and tetraodontiform swimmers (Supplementary Table S3). The labriform swimmer anal fin morphospace is 81%–82% unique from benthic species and tetraodontiform swimmers.

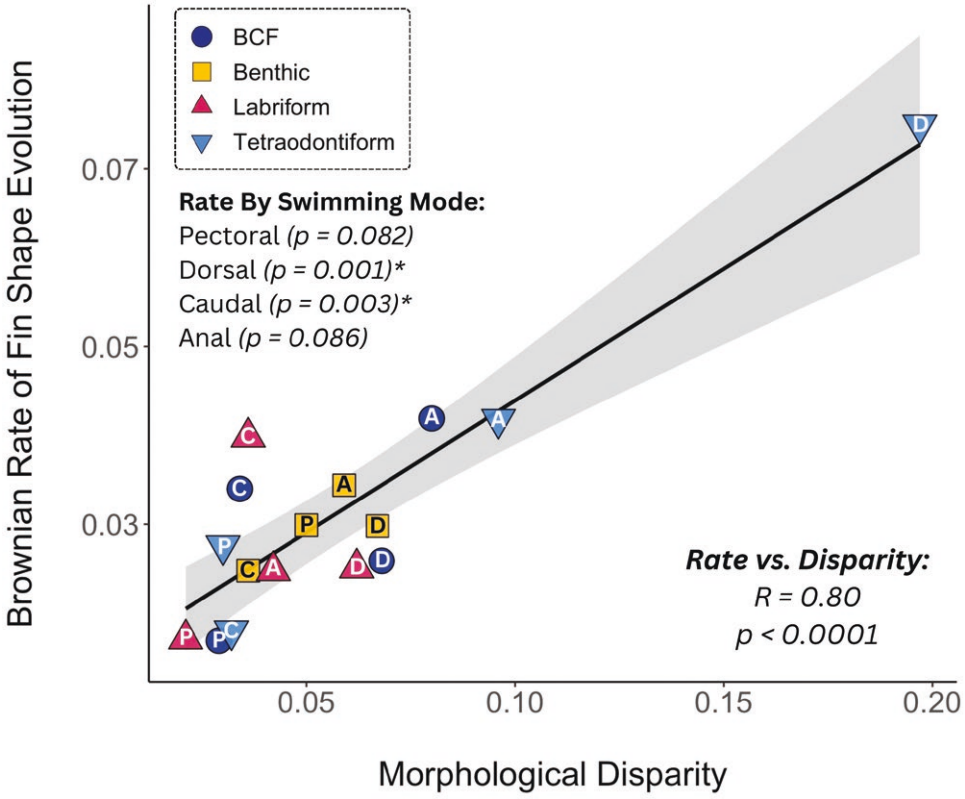

Figure 7. Brownian rate of fin shape evolution versus morphological disparity. For each fin, the Brownian rate of fin shape evolution and morphological disparity were calculated within locomotor mode groups using *geomorph (v 4.0.5; R)*. Rates have been multiplied by 10,000. Dark blue circles represent body-caudal fin swimmers, yellow squares represent benthic species, magenta triangles represent labriform swimmers, and light blue inverted triangles represent tetraodontiform swimmers. Points are labeled with the first letter of the fin type that they represent, such that pectoral fin points are labeled "P." The correlation coefficient (*R*) and the associated *p*-value for the relationship between rate and disparity are provided. *p* values next to the fin names indicate the effect of locomotor mode on the rate of evolution within that fin type, and significant *p* values are indicated with asterisks. Rates of fin evolution and disparity are correlated. The tetraodontiform dorsal evolves exceptionally fast, and the pectoral fin is the slowest evolving fin on average.

However, roughly 55% of the benthic species' and 50% of the tetraodontiform species' volumes overlap with the labriform volume (Supplementary Table S3). All other pectoral, caudal, dorsal, or anal comparisons not explicitly mentioned above were highly overlapping in hypervolume space.

Effects of swimming mode on fin shape evolutionary integration and rate of evolution

To understand if fins are evolutionarily correlated, we tested for phylogenetic integration in the fins across all species. Among all species, we find that all fins are integrated (r = 0.32–0.61, Z = 1.95–4.90, p = 0.001–0.023, df = 105) except for the pectoral and dorsal (r = 0.30, Z = 1.24, p = 0.116, df = 1,105; Figure 6; Table 3). Elongate, wing-like pectorals typically occur with more forked caudals and elongate, low-lying anal and dorsal fins, while rounded, paddle-like pectorals occur with rounded caudals and short and deep anal and dorsal fins (Figure 6A–C). Low-lying, elongate dorsal fins are more common with more forked caudals and elongate, low-lying anal fins (Figure 6D and E). Rounded caudals occur with deeper, short anal fins, while more forked caudals occur with elongate, low-lying anal fins (Figure 6F). While these overall axes of fin covariation (Figure 6 black dashed lines) act as overarching pipelines of diversification, there is much diversity within locomotor groups that is accumulated off-axis of the primary axis of covariation (Figure 6 colored solid lines).

To determine if patterns of fin evolutionary integration shift with the evolution of novel swimming modes, we tested for phylogenetic integration among the fins of species within swimming groups (Figures 5 and 6; Table 3). This analysis allows us to compare patterns of trait covariation when species are evolving in the ancestral state, BCF swimming, to trait covariation among species that have evolved a novel swimming mode. We find that fin modules among BCF swimming reef fishes are more integrated than any of the derived swimming modes. In BCF swimmers, all fins are integrated except for the pectoral and dorsal (p = 0.149, df = 1,105), with the most substantial integration being between the dorsal and anal fins (r = 0.70, Z = 3.76, p = 0.001, df = 1,105; Figure 5; Table 3). Aside from the dorsal-anal integration, the BCF fin integrations are significant but relatively weak, with a correlation coefficient (r) ranging from 0.45 to 0.54 and effect sizes (Z) from 1.67 to 2.32 (p = 0.008–0.047, df = 105; Figure 5; Table 3). The dorsal and anal remain integrated in the three derived swimming modes, though with a weaker signal (r = 0.65–0.90, Z = 2.17–2.68, p = 0.005–0.022, df = 105; Figure 5; Table 3). All other axes of integration have been lost in all three derived swimming modes (Table 3; p = 0.050–0557, Z = –0.14 to 1.77, df = 105; Figure 5; Table 3). Figure 5 illustrates the effect sizes (Z) of the phylogenetic integration tests, showing that in all cases where there is a significant effect of integration for BCF swimmers (excluding the pectoral-dorsal pair), the strength of integration decreases with the evolution

of benthic, labriform, and tetraodontiform swimming. These findings suggest that fins evolve with more independence following the evolution of novel swimming modes. We note that some caution is warranted with this result as an increase in the number of species sampled could lead to more significant integration between fins in the derived swimming modes.

Rates of evolution among reef fish fins are variable across fin types and across swimming groups, further indicating that fins and swimming groups show different evolutionary patterns. When comparing the Brownian rates of fin shape evolution for all species, we find a rate ratio of 2.6 ($Z = 18.98$, $p = 0.001$, $df = 3{,}105$), where the dorsal fin is evolving the fastest (rate = 3.17×10^{-4}) and the pectoral has the slowest rate (rate = 1.25×10^{-4}). The caudal (rate = 2.54×10^{-4}) and anal (1.71×10^{-4}) are intermediate in the Brownian rate of evolution. Much of the high rate in the dorsal fin comes from the vast morphological disparity acquired by tetraodontiform fishes in a relatively short amount of time ($p = 0.001$, $df = 3{,}105$; Figure 7). In addition to the dorsal fin, the caudal fin also shows a significant effect of swimming mode on the rate of evolution, where BCF and labriform swimmers have caudals that evolve faster than tetraodontiform or benthic species ($p = 0.003$, $df = 3{,}105$; Figure 7). While we detected no significant effect of swimming mode on the rate of evolution in the pectoral fins ($p = 0.082$, $df = 3{,}105$; Figure 7), it is notable that BCF and labriform swimmers have low rates of evolution relative to tetraodontiform and benthic species. BCF, benthic, and tetraodontiform swimmers have similar rates of evolution of the anal fin, and the rate is lower for labriform swimmers though not statistically so ($p = 0.086$, $df = 3{,}105$; Figure 7).

Discussion

Locomotor diversity relates broadly to reef fish ecology, including feeding, habitat use, and reproduction. However, the locomotor system in reef fishes is complex and comprises many fins, all of which may directly and indirectly be subject to selection for locomotor specialization. Previous studies have described varying levels of functional cooperation between the fins of reef fishes (Blake, 2004; Fulton, 2007; Sfakiotakis et al., 1999), ecological specialization of the fins (Bellwood & Wainwright, 2001; Bridge et al., 2016), and shared physical and genetic developmental pathways among fins (Ahn et al., 2002; Crotwell & Mabee, 2007; Crotwell et al., 2001, 2004; Dahn et al., 2007; Freitas et al., 2006; Goodrich, 1906; Heude et al., 2014; Letelier et al., 2018; Mabee et al., 2002; Neumann et al., 1999; Sordino et al., 1995). Each of these factors has the potential to strongly influence the macroevolutionary patterns of fin diversification and points toward an expectation of strong integration among fins. In contrast to this expectation, we find only a weak relationship between swimming mode and fin shape and unexpected diversity of fins within each swimming mode category. In their ancestral swimming condition, reef fishes exhibit significant but weak integration among fins, which is weakened with the introduction of derived swimming modes. These and other findings are discussed below.

Weak signals of swimming mode in fin morphospace occupation and evolutionary rate

Relationships between form and function are often the core focus for evolutionary biologists aiming to describe mechanisms driving the accumulation of diversity in highly diverse functional systems. In locomotor systems, differences among taxa in routine locomotor mode are often related to diversity in limb anatomy (Berman, 1985; Buttimer et al., 2020; Citadini et al., 2018; Martín-Serra et al., 2014; Wainwright et al., 2002). However, in reef fishes, we find swimming mode diversity is not a strong predictor of fin shape. In each fin we measured there are large areas of overlap where multiple swimming groups occupy similar fin shapes. Further, the range of fin shapes that each swimming group contains is typically quite expansive. For example, the caudal fins of benthic species, BCF, and labriform swimmers span the full axis of rounded to forked, and the dorsal and anal fin diversity of benthic and labriform swimmers is almost entirely nested inside the diversity of BCF swimmers. As such, if one selected a caudal, dorsal, or anal fin shape at random, it would be a challenge to identify which swimming group the fin belonged to. This observation is counter to an expectation of strong links between swimming mode and fin shape and suggests a reevaluation of the relationship is warranted.

Pectoral fins show the strongest signal of swimming mode effects, as benthic species have pectoral fins with trailing edge rays that are more elongate than other groups (Figure 2, Table 1), and the hypervolumes show that a large region of pectoral fin morphospace is only accessible to benthic species (Figure 4; Table 2). The comparisons between focal swimming groups versus all other species showed that BCF, labriform, and tetraodontiform pectoral fins are notably excluded from much of the morphospace occupied by other species. In particular, the average BCF pectoral is generally confined to regions of more elongate shapes with rays that are longest in the middle of the fin relative to the labriform and tetraodontiform groups that have more rounded pectorals where the longest ray is along the leading edge. Note that the pectoral fin is the most important fin in labriform propulsion, and the finding that the labriform pectoral fin occupies less unique space than expected under a null model (Table 2) and the low Brownian rate of evolution and low disparity (Figure 7; Supplementary Table S2) suggests that the functional role of the pectoral in labriform swimming may constrain its morphospace diversification. In contrast to labriform species in which the pectoral is the predominant propulsor and shows reduced rates of evolution and disparity, benthic species do not extensively use their pectoral fins for locomotion but rather for stabilization via substrate contact. Lacking the functional constraints of locomotor function and with novel demands for physically interacting with the substrate, pectoral fins in benthic species evolve relatively rapidly with high morphological disparity (Figure 7; Supplementary Table S2).

Tetraodontiform locomotion is highly reliant on the cooperation between the dorsal and anal fins. In this group, we find that both fins occupy a region of morphospace that is shorter in base length and deeper on average than other locomotor modes. We also find that in hypervolume analyses a significant region of the tetraodontiform anal and dorsal fins are unique from all other species. However, there remains a substantial morphological disparity in the tetraodontiform locomotor fins, in part because the families Balistidae and Monocanthidae have evolved a split dorsal fin in which the spiny region of the fin is not used in locomotion but is rather a predominant anti-predator defense structure (Matsuura, 1979). The disparity in the tetraodontiform anal fin reflects diversity in the lengthening of different regions of the anal fin. Specifically, balistids and monacanthids have longer anterior edges which may reflect a genetic or developmental

lack of independence with the elongation of the spiny first dorsal (Sorenson, 2007). It is plausible that if one examined the rate of evolution and morphological disparity of only the soft ray dorsal fin in tetraodontiform swimmers, it would be more reflective of the rate and disparity in the anal fin. Future work should be done to investigate the functional decoupling of the first and second dorsal fin and the implication of that decoupling for locomotor evolution. Interestingly, the caudal and pectoral fins in tetraodontiform swimmers occupy narrow regions of morphospace and have low rates of evolution, possibly reflecting limited selective pressure to evolve outside of the existing diversity in this clade. However, many species in this group feed on benthic invertebrates, requiring the ability to navigate complex benthic structures (Corn et al., 2022; Turingan, 1994). Thus, the confinement to a narrow morphospace in the tetraodontiform caudal and pectoral could reflect constraints induced by their essential role in maneuvering and stabilization (Blake, 1978; Dornburg et al., 2011).

We found only subtle evidence of the role of fin shape diversity in locomotor variation. Similar results have been observed outside of reef-dwelling acanthomorphs. For example, in selachimorph elasmobranchs studies have found a large degree of overlap in pectoral and dorsal fin shape across ecomorphs (Hoffman et al., 2020; Irschick et al., 2017). In contrast, the selachimorph caudal fin shape displays higher variance among distantly related species and is a moderate correlate of swimming speed (Iliou et al., 2023; Irschick et al., 2017). In cichlids, there is a high degree of disparity in fin shape, though most clades overlap in morphospace (Feilich, 2016). Evidence of relationships between fin shape and function in cichlids is limited to a slight tendency for benthic species to have larger area pectorals, though no difference in caudal fin area by habitat type was observed (Colombo et al., 2016). Thus, it may be a general pattern that fish fin shape variation is weakly if at all predictive of locomotor diversity at broad taxonomic scales.

Evolutionary integration between fins is lost with locomotor expansion

Evolutionary integration has been debated as either a facilitator or hinderer of diversification in complex functional systems (Burns et al., 2023; Du et al., 2019; Eliason et al., 2023; Evans et al., 2017, 2021; Felice et al., 2018; Goswami & Polly, 2010; Hansen, 2003; Larouche et al., 2018; Marroig et al., 2009). In the vertebrate locomotor system, the typical ancestral condition is one of functional cooperation among the limbs, which, in combination with shared genetic and developmental limb origins, can induce evolutionary integration (Gatesy & Dial, 1996; Goswami et al., 2014; Hallgrímsson et al., 2002; Petit et al., 2017; Wimberly et al., 2021). Reef fishes appear to follow this general rule as we find that the most likely ancestral state is BCF swimming, which makes use of all fins more regularly than derived swimming modes. We observe that across all species almost all fin combinations are integrated (Table 3 grey column). However, when we parse our group of reef fishes into swimming categories, we find that patterns of integration in reef fishes are largely driven by the integration that is present among BCF swimming fish and when novel swimming modes evolve, integration among fins is lost almost entirely (Table 3).

Integration in the ancestral swimming mode is expected given that the caudal, dorsal, and anal fins are developmentally linked by origination in a common fin fold. Though the pectoral is spatially isolated from the other fins there are common genetic pathways across all fins regulating the generation of fin buds, supports, soft tissue, and rays (Ahn et al., 2002; Crotwell & Mabee, 2007; Crotwell et al., 2001, 2004; Dahn et al., 2007; Heude et al., 2014; Letelier et al., 2018; Sordino et al., 1995). Unexpectedly the significant integration present in BCF swimmers is not overwhelmingly strong (mean $r = 0.52$, mean $Z = 2.19$), allowing for the evolution of a large amount of off-axis diversity in fin shape. Further, the different rates of fin shape evolution and the spectrum of accumulated morphological disparity (Figure 7) suggest considerable independent evolution of fin shape even in the ancestral swimming mode. Together, these findings indicate that for reef fishes, weak to moderate ancestral integration acted as an evolutionary pathway of least resistance, reflecting a predominant axis for diversification while allowing for exploration of off-axis regions of morphospace.

We additionally find that reef fishes experience locomotor expansion through lability in evolutionary integration (Table 3, Figure 5). We find that with each novel swimming mode (labriform, tetraodontiform, and benthic) that arises out of BCF swimming, there is a loss of detectible evolutionary integration between most of the fins. Our findings mirror patterns observed in birds and mammals in which locomotor expansion into bipedal walking and flight consistently co-occur with the reduction in morphological correlation between limbs (Bell et al., 2011; Garland et al., 2017; Goswami et al., 2014; Kelly & Sears, 2011; Young & Hallgrímsson, 2005; Young et al., 2010). For reef fishes this secondary breakdown of integration with locomotor diversification allowed fins to independently evolve and further access disparate regions of morphospace. This pattern is particularly evident in the rounding and trailing edge elongation of the pectoral fin following the evolution of benthic ecology, and the deepening of the dorsal and anal fins in Tetraodontiforms. We note that the loss of integration between fins in derived swimming modes should be viewed with some caution as the differences in estimated correlations are subtle and larger samples of species could change this result. Though there is a loss of significance in the integration following evolutions of novel swimming modes, often the value of the correlation (r) remains similar to, or in some cases is greater than, the value in BCF swimmers. As such, it is possible that the loss of detectable integration among fins in derived swimming modes is a product of smaller sample sizes.

Evolutionary correlation among fins has also been found in cichlids (Feilich, 2016). The strongest correlation we observe among all the reef fishes included in this study was between the dorsal and anal fin ($r = 0.61$). Meanwhile, the evolutionary correlation between the caudal, dorsal, and anal fins in cichlids ranges from $r = 0.69$ to 0.88. The integration between the dorsal and anal fins is also strongest in cichlids, though pectoral fins were not included (Feilich, 2016). The axes of integration we find in reef fishes, and those which have been found in cichlids align with functional trade-offs, where species evolve along a spectrum of deep, rounded, low AR fins suitable for maneuverability and power to elongate, pointed, high AR fins better for efficient high-speed swimming (Bellwood & Wainwright, 2001; Bridge et al., 2016; Drucker & Lauder, 2002; Standen & Lauder, 2005; Wainwright et al., 2002; Walker & Westneat, 2002). Though patterns of *fin shape* integration have not

been evaluated for other groups of fishes, across a broader range of actinopterygians (Larouche et al., 2018) and within the damselfish family, Pomacentridae, (Aguilar-Medrano et al., 2016) models of modularity support independent evolution of the caudal region (including the insertions of the caudal fin) relative to the trunk of the body (including the insertions of the MPF). A separation of the median-paired fins and the caudal into distinct modules may also reflect locomotor specialization on a spectrum of maneuverability to economic swimming. Our analyses of reef fishes indicate that patterns of integration are more evolutionarily labile than previously appreciated and it is possible that comparing patterns of integration among the fins across additional clades of fishes and at a range of taxonomic scales may uncover a more detailed history of fin covariation through fish diversification.

Conclusion

The effect of swimming mode on reef fish fin morphospace is limited, as there is high diversity in fin morphology within swimming groups. The many-to-one mapping of fin shape to swimming mode demonstrates that no single fin shape is most suited to satisfying the demands of any specific swimming style. We find that fin shape diversity exists within the context of many axes of weak to moderate integration among fins particularly in the ancestral swimming condition, BCF swimming. These mild axes of integration reflect primary axes of diversification in reef fish fin evolution while allowing for some movement into regions of morphospace not aligned with axes of covariation. We observe the loss of evolutionary integration between fins with each evolution of novel swimming modes, allowing for morphological expansion into farther reaches of the morphospace. As similar patterns have been hinted at in mammals and birds (though not yet confirmed with comparative phylogenetic methods), we predict that weak ancestral integration among locomotor modules followed by diversification of locomotor modes through the weakening or loss of evolutionary integration is prevalent across vertebrates.

Supplementary material

Supplementary material is available online at *Evolution*.

Data availability

Data and code are available through DataDryad.org at DOI: 10.5061/dryad.crjdfn3dm.

Author contributions

D.R. Satterfield designed study questions and data collection protocol, photographed specimens, collected data from photographs, and led analyses and writing. P.C. Wainwright advised on study design, procured specimens, prepared specimens, and advised on analyses. M.D. Burns advised on analyses and conceptual framework. B. Yin, S. Jung, and S. Hodges-Lisk photographed specimens. D.K. Wainwright procured specimens, prepared specimens, and advised on study design.

Funding

DRS was supported by the University of California, Office of the President's Pre-Professoriate Fellowship. This project was supported by the University of California Davis, Center for Population Biology and grant No. DEB-1556953 from the National Science Foundation to PCW.

Conflict of interest: Authors have no conflicts of interest to report.

Acknowledgments

We thank D. Adams, K. Corn, A. Roberts, S. Freidman, M. Mihalitsis, and N. Peoples for their guidance on statistical analyses and feedback. Animal handling and care procedures followed protocol No. 22206 with the Institutional Animal Care and Use Committee.

References

Adams, D. C., & Collyer, M. L. (2019). Comparing the strength of modular signal, and evaluating alternative modular hypotheses, using covariance ratio effect sizes with morphometric data. *Evolution*, *73*(12), 2352–2367. https://doi.org/10.1111/evo.13867

Adams, D. C., Collyer, M. L., Kaliontzopoulou, A., & Baken, E. K. (2024). *Geomorph: Software for geometric morphometric analyses* (R package version 4.0.8). https://cran.r-project.org/package=geomorph

Aguilar-Medrano, R., Frédérich, B., & Barber, P. H. (2016). Modular diversification of the locomotor system in damselfishes (Pomacentridae). *Journal of Morphology*, *277*(5), 603–614. https://doi.org/10.1002/jmor.20523

Ahn, D., Kourakis, M. J., Rohde, L. A., Silver, L. M., & Ho, R. K. (2002). T-box gene tbx5 is essential for formation of the pectoral limb bud. *Nature*, *417*(6890), 754–758. https://doi.org/10.1038/nature00814

Baken, E. K., Collyer, M. L., Kaliontzopoulou, A., & Adams, D. C. (2021). geomorph v4.0 and gmShiny: Enhanced analytics and a new graphical interface for a comprehensive morphometric experience. *Methods in Ecology and Evolution*, *12*(12), 2355–2363. https://doi.org/10.1111/2041-210x.13723

Beaulieu, J. M., Jhwueng, D. -C., Boettiger, C., & O'Meara, B. C. (2012). Modeling stabilizing selection: Expanding the Ornstein-Uhlenbeck model of adaptive evolution. *Evolution*, *66*(8), 2369–2383. https://doi.org/10.1111/j.1558-5646.2012.01619.x

Bell, E., Andres, B., & Goswami, A. (2011). Integration and dissociation of limb elements in flying vertebrates: A comparison of pterosaurs, birds and bats. *Journal of Evolutionary Biology*, *24*(12), 2586–2599. https://doi.org/10.1111/j.1420-9101.2011.02381.x

Bellwood, D. R., Goatley, C. H. R., Brandl, S. J., & Bellwood, O. (2014). Fifty million years of herbivory on coral reefs: Fossils, fish and functional innovations. *Proceedings of the Royal Society B: Biological Sciences*, *281*(1781), 20133046. https://doi.org/10.1098/rspb.2013.3046

Bellwood, D. R., Hoey, A. S., Bellwood, O., & Goatley, C. H. R. (2014). Evolution of long-toothed fishes and the changing nature of fish–benthos interactions on coral reefs. *Nature Communications*, *5*(1), 3144. https://doi.org/10.1038/ncomms4144

Bellwood, D. R., & Wainwright, P. C. (2001). Locomotion in labrid fishes: Implications for habitat use and cross-shelf biogeography on the Great Barrier Reef. *Coral Reefs*, *20*(2), 139–150. https://doi.org/10.1007/s003380100156

Bellwood, D. R., & Wainwright, P. C. (2002). The history and biogeography of fishes on coral reefs. In P. F. Sale (Ed.), *Coral reef fishes: Dynamics and diversity in a complex ecosystem* (pp. 5–32). Academic Press.

Berman, S. L. (1985). Convergent evolution in the hindlimb of bipedal rodents. *Journal of Zoological Systematics and Evolutionary Research*, *23*(1), 59–77. https://doi.org/10.1111/j.1439-0469.1985.tb00570.x

Blake, R. W. (1978). On balistiform locomotion. *Journal of the Marine Biological Association of the United Kingdom*, *58*(1), 73–80. https://doi.org/10.1017/s0025315400024401

Blake, R. W. (2004). Fish functional design and swimming performance. *Journal of Fish Biology*, *65*(5), 1193–1222. https://doi.org/10.1111/j.0022-1112.2004.00568.x

Blonder, B., Morrow, with contributions from C. B., Brown, S., Butruille, G., Chen, D., Laini, A., & Harris, and D. J. (2023). *hypervolume: High Dimensional Geometry, Set Operations, Projection, and Inference Using Kernel Density Estimation, Support Vector Machines, and Convex Hulls (3.1.3)*. https://cran.r-project.org/web/packages/hypervolume/index.html

Breder, C. M. (1926). The locomotion of fishes. *Zoologica*, *4*(5), 159–297. https://doi.org/10.5962/p.203769

Bridge, T. C. L., Luiz, O. J., Coleman, R. R., Kane, C. N., & Kosaki, R. K. (2016). Ecological and morphological traits predict depth-generalist fishes on coral reefs. *Proceedings of the Royal Society B: Biological Sciences*, *283*(1823), 20152332. https://doi.org/10.1098/rspb.2015.2332

Burns, M. D., Collyer, M. L., & Sidlauskas, B. L. (2023). Simultaneous integration and modularity underlie the exceptional body shape diversification of characiform fishes. *Evolution*, *77*(3), 746–762. https://doi.org/10.1093/evolut/qpac070

Burns, M. D., Satterfield, D. R., Peoples, N., Chan, H., Barley, A. J., Roberts-Hugghis, A., Russell, K. T., Hess, M., Williamson, S., Corn, K. A., Mihalitsis, M., Wainwright, D. K., & Wainwright, P. C. (2024). Complexity and weak integration promote the diversity of reef fish oral jaws. *Communications Biology*, *7*(1), 1–13.

Buttimer, S. M., Stepanova, N., & Womack, M. C. (2020). Evolution of the unique anuran pelvic and hind limb skeleton in relation to microhabitat, locomotor mode, and jump performance. *Integrative and Comparative Biology*, *60*(5), 1330–1345. https://doi.org/10.1093/icb/icaa043

Chang, J., Rabosky, D. L., Smith, S. A., & Alfaro, M. E. (2019). An r package and online resource for macroevolutionary studies using the ray-finned fish tree of life. *Methods in Ecology and Evolution*, *10*(7), 1118–1124. https://doi.org/10.1111/2041-210x.13182

Citadini, J. M., Brandt, R., Williams, C. R., & Gomes, F. R. (2018). Evolution of morphology and locomotor performance in anurans: Relationships with microhabitat diversification. *Journal of Evolutionary Biology*, *31*(3), 371–381. https://doi.org/10.1111/jeb.13228

Collyer, M. L., & Adams, D. C. (2018). RRPP: An r package for fitting linear models to high-dimensional data using residual randomization. *Methods in Ecology and Evolution*, *9*(7), 1772–1779. https://doi.org/10.1111/2041-210x.13029

Collyer, M. L., & Adams, D. C. (2024). Rrpp: Linear model evaluation with randomized residuals in a permutation procedure (2.0.0). https://cran.r-project.org/web/packages/RRPP/index.html

Colombo, M., Indermaur, A., Meyer, B. S., & Salzburger, W. (2016). Habitat use and its implications to functional morphology: Niche partitioning and the evolution of locomotory morphology in Lake Tanganyikan cichlids (Perciformes: Cichlidae). *Biological Journal of the Linnean Society*, *118*(3), 536–550. https://doi.org/10.1111/bij.12754

Corn, K. A., Friedman, S. T., Burress, E. D., Martinez, C. M., Larouche, O., Price, S. A., & Wainwright, P. C. (2022). The rise of biting during the Cenozoic fueled reef fish body shape diversification. *Proceedings of the National Academy of Sciences of the United States of America*, *119*(31), e2119828119. https://doi.org/10.1073/pnas.2119828119

Crotwell, P. L., Clark, T. G., & Mabee, P. M. (2001). Gdf5 is expressed in the developing skeleton of median fins of late-stage zebrafish, *Danio rerio*. *Development Genes and Evolution*, *211*(11), 555–558. https://doi.org/10.1007/s00427-001-0186-z

Crotwell, P. L., & Mabee, P. M. (2007). Gene expression patterns underlying proximal–distal skeletal segmentation in late-stage zebrafish, *Danio rerio*. *Developmental Dynamics*, *236*(11), 3111–3128. https://doi.org/10.1002/dvdy.21352

Crotwell, P. L., Sommervold, A. R., & Mabee, P. M. (2004). Expression of bmp2a and bmp2b in late-stage zebrafish median fin development. *Gene Expression Patterns: GEP*, *5*(2), 291–296. https://doi.org/10.1016/j.modgep.2004.07.001

Crumière, A. J. J., Santos, M. E., Sémon, M., Armisén, D., Moreira, F. F. F., & Khila, A. (2016). Diversity in morphology and locomotory behavior is associated with niche expansion in the semi-aquatic bugs. *Current Biology: CB*, *26*(24), 3336–3342. https://doi.org/10.1016/j.cub.2016.09.061

Dahn, R. D., Davis, M. C., Pappano, W. N., & Shubin, N. H. (2007). Sonic hedgehog function in chondrichthyan fins and the evolution of appendage patterning. *Nature*, *445*(7125), 311–314. https://doi.org/10.1038/nature05436

Di Santo, V., Goerig, E., Wainwright, D. K., Akanyeti, O., Liao, J. C., Castro-Santos, T., & Lauder, G. V. (2021). Convergence of undulatory swimming kinematics across a diversity of fishes. *Proceedings of the National Academy of Sciences of the United States of America*, *118*(49), e2113206118. https://doi.org/10.1073/pnas.2113206118

Dingerkus, G., & Uhler, L. D. (1977). Enzyme clearing of alcian blue stained whole small vertebrates for demonstration of cartilage. *Stain Technology*, *52*(4), 229–232. https://doi.org/10.3109/10520297709116780

Dornburg, A., Sidlauskas, B., Santini, F., Sorenson, L., Near, T. J., & Alfaro, M. E. (2011). The influence of an innovative locomotor strategy on the phenotypic diversification of triggerfish (family: Balistidae). *Evolution*, *65*(7), 1912–1926. https://doi.org/10.1111/j.1558-5646.2011.01275.x

Drucker, E. G., & Lauder, G. V. (2002). Wake dynamics and locomotor function in fishes: Interpreting evolutionary patterns in pectoral fin design. *Integrative and Comparative Biology*, *42*(5), 997–1008. https://doi.org/10.1093/icb/42.5.997

Du, T. Y., Tissandier, S. C., & Larsson, H. C. E. (2019). Integration and modularity of teleostean pectoral fin shape and its role in the diversification of acanthomorph fishes. *Evolution*, *73*(2), 401–411. https://doi.org/10.1111/evo.13669

Eliason, C. M., Proffitt, J. V., & Clarke, J. A. (2023). Early diversification of avian limb morphology and the role of modularity in the locomotor evolution of crown birds. *Evolution*, *77*(2), 342–354. https://doi.org/10.1093/evolut/qpac039

Essner, R. L. Jr. (2007). Morphology, locomotor behaviour and microhabitat use in North American squirrels. *Journal of Zoology*, *272*(1), 101–109. https://doi.org/10.1111/j.1469-7998.2006.00247.x

Evans, K. M., Buser, T. J., Larouche, O., & Kolmann, M. A. (2023). Untangling the relationship between developmental and evolutionary integration. *Seminars in Cell & Developmental Biology*, *145*, 22–27. https://doi.org/10.1016/j.semcdb.2022.05.026

Evans, K. M., Larouche, O., Watson, S. -J., Farina, S., Habegger, M. L., & Friedman, M. (2021). Integration drives rapid phenotypic evolution in flatfishes. *Proceedings of the National Academy of Sciences of the United States of America*, *118*(18), e2101330118. https://doi.org/10.1073/pnas.2101330118

Evans, K. M., Waltz, B. T., Tagliacollo, V. A., Sidlauskas, B. L., & Albert, J. S. (2017). Fluctuations in evolutionary integration allow for big brains and disparate faces. *Scientific Reports*, *7*(1), Article 1. https://doi.org/10.1038/srep40431

Feilich, K. L. (2016). Correlated evolution of body and fin morphology in the cichlid fishes. *Evolution*, *70*(10), 2247–2267. https://doi.org/10.1111/evo.13021

Felice, R. N., Randau, M., & Goswami, A. (2018). A fly in a tube: Macroevolutionary expectations for integrated phenotypes. *Evolution*, *72*(12), 2580–2594. https://doi.org/10.1111/evo.13608

Freitas, R., Zhang, G., & Cohn, M. J. (2006). Evidence that mechanisms of fin development evolved in the midline of early vertebrates. *Nature*, *442*(7106), 1033–1037. https://doi.org/10.1038/nature04984

Fulton, C., Bellwood, D., & Wainwright, P. (2001). The relationship between swimming ability and habitat use in wrasses

(Labridae). *Marine Biology*, *139*(1), 25–33. https://doi.org/10.1007/s002270100565

Fulton, C. J. (2007). Swimming speed performance in coral reef fishes: Field validations reveal distinct functional groups. *Coral Reefs*, *26*(2), 217–228. https://doi.org/10.1007/s00338-007-0195-0

Garland, K., Marcy, A., Sherratt, E., & Weisbecker, V. (2017). Out on a limb: Bandicoot limb co-variation suggests complex impacts of development and adaptation on marsupial forelimb evolution. *Evolution & Development*, *19*(2), 69–84. https://doi.org/10.1111/ede.12220

Gatesy, S. M., & Dial, K. P. (1996). Locomotor modules and the evolution of avian flight. *Evolution*, *50*(1), 331–340. https://doi.org/10.1111/j.1558-5646.1996.tb04496.x

Gatesy, S. M., & Middleton, K. M. (1997). Bipedalism, flight, and the evolution of theropod locomotor diversity. *Journal of Vertebrate Paleontology*, *17*(2), 308–329. https://doi.org/10.1080/02724634.1997.10010977

Goodrich, E. S. (1906). Notes on the development, structure, and origin of the median and paired fins of fish. *Journal of Cell Science*, *S2-50*(198), 333–376. https://doi.org/10.1242/jcs.s2-50.198.333

Goswami, A., & Polly, P. D. (2010). The influence of modularity on cranial morphological disparity in carnivora and primates (Mammalia). *PLoS One*, *5*(3), e9517. https://doi.org/10.1371/journal.pone.0009517

Goswami, A., Smaers, J. B., Soligo, C., & Polly, P. D. (2014). The macroevolutionary consequences of phenotypic integration: From development to deep time. *Philosophical Transactions of the Royal Society of London, Series B: Biological Sciences*, *369*(1649), 20130254. https://doi.org/10.1098/rstb.2013.0254

Granatosky, M. C. (2018). A review of locomotor diversity in mammals with analyses exploring the influence of substrate use, body mass and intermembral index in primates. *Journal of Zoology*, *306*(4), 207–216. https://doi.org/10.1111/jzo.12608

Hallgrímsson, B., Willmore, K., & Hall, B. K. (2002). Canalization, developmental stability, and morphological integration in primate limbs. *American Journal of Physical Anthropology*, *119*(S35), 131–158. https://doi.org/10.1002/ajpa.10182

Hansen, T. F. (2003). Is modularity necessary for evolvability? Remarks on the relationship between pleiotropy and evolvability. *Biosystems*, *69*(2–3), 83–94. https://doi.org/10.1016/s0303-2647(02)00132-6

Harris, J. E. (1937). *The mechanical significance of the position and movements of the paired fins in the teleostei*. Carnegie Institution of Washington.

Heude, E., Shaikho, S., & Ekker, M. (2014). The dlx5a/dlx6a genes play essential roles in the early development of zebrafish median fin and pectoral structures. *PLoS One*, *9*(5), e98505. https://doi.org/10.1371/journal.pone.0098505

Hoffmann, S. L., Buser, T. J., & Porter, M. E. (2020). Comparative morphology of shark pectoral fins. *Journal of Morphology*, *281*(11), 1501–1516. https://doi.org/10.1002/jmor.21269

Iliou, A. S., Vanderwright, W., Harding, L., Jacoby, D. M. P., Payne, N. L., & Dulvy, N. K. (2023). Tail shape and the swimming speed of sharks. *Royal Society Open Science*, *10*(10), 231127. https://doi.org/10.1098/rsos.231127

Irschick, D. J., Fu, A., Lauder, G., Wilga, C., Kuo, C. -Y., & Hammerschlag, N. (2017). A comparative morphological analysis of body and fin shape for eight shark species. *Biological Journal of the Linnean Society*, *122*(3), 589–604. https://doi.org/10.1093/biolinnean/blx088

Kelly, M. E., & Sears, K. E. (2011). Reduced phenotypic covariation in marsupial limbs and the implications for mammalian evolution. *Biological Journal of the Linnean Society*, *102*(1), 22–36. https://doi.org/10.1111/j.1095-8312.2010.01561.x

Klingenberg, C. P. (2008). Morphological integration and developmental modularity. *Annual Review of Ecology, Evolution, and Systematics*, *39*(1), 115–132. https://doi.org/10.1146/annurev.ecolsys.37.091305.110054

Korsmeyer, K. E., Steffensen, J. F., & Herskin, J. (2002). Energetics of median and paired fin swimming, body and caudal fin swimming, and gait transition in parrotfish (*Scarus schlegeli*) and triggerfish (*Rhinecanthus aculeatus*). *The Journal of Experimental Biology*, *205*(Pt 9), 1253–1263. https://doi.org/10.1242/jeb.205.9.1253

Larouche, O., Zelditch, M. L., & Cloutier, R. (2018). Modularity promotes morphological divergence in ray-finned fishes. *Scientific Reports*, *8*(1), Article 1. https://doi.org/10.1038/s41598-018-25715-y

Lauder, G. V., & Drucker, E. G. (2004). Morphology and experimental hydrodynamics of fish fin control surfaces. *IEEE Journal of Oceanic Engineering*, *29*(3), 556–571. https://doi.org/10.1109/joe.2004.833219

Letelier, J., de la Calle-Mustienes, E., Pieretti, J., Naranjo, S., Maeso, I., Nakamura, T., Pascual-Anaya, J., Shubin, N. H., Schneider, I., Martinez-Morales, J. R., & Gómez-Skarmeta, J. L. (2018). A conserved Shh cis-regulatory module highlights a common developmental origin of unpaired and paired fins. *Nature Genetics*, *50*(4), 504–509. https://doi.org/10.1038/s41588-018-0080-5

Lindsey, C. C. (1978). Form, function, and locomotory habits in fish. In W. S. Hoar, & D. J. Randall (Eds.), *Fish physiology* (Vol. 7, pp. 1–100). Academic Press. https://doi.org/10.1016/S1546-5098(08)60163-6

Mabee, P. M., Crotwell, P. L., Bird, N. C., & Burke, A. C. (2002). Evolution of median fin modules in the axial skeleton of fishes. *The Journal of experimental zoology*, *294*(2), 77–90. https://doi.org/10.1002/jez.10076

MacArthur, R. H. (1957). On the relative abundance of bird species. *Proceedings of the National Academy of Sciences of the United States of America*, *43*(3), 293–295. https://doi.org/10.1073/pnas.43.3.293

Marroig, G., Shirai, L. T., Porto, A., de Oliveira, F. B., & De Conto, V. (2009). The evolution of modularity in the mammalian skull II: Evolutionary consequences. *Evolutionary Biology*, *36*(1), 136–148. https://doi.org/10.1007/s11692-009-9051-1

Martín-Serra, A., Figueirido, B., & Palmqvist, P. (2014). A three-dimensional analysis of morphological evolution and locomotor performance of the carnivoran forelimb. *PLoS One*, *9*(1), e85574. https://doi.org/10.1371/journal.pone.0085574

Matsuura, K. (1979). Phylogeny of the superfamily Balistoidea (Pisces: Tetraodontiformes). *Memoirs of the Faculty of Fisheries Hokkaido University*, *26*(1–2), 49–169.

McCord, C. L., Nash, C. M., Cooper, W. J., & Westneat, M. W. (2021). Phylogeny of the damselfishes (Pomacentridae) and patterns of asymmetrical diversification in body size and feeding ecology. *PLoS One*, *16*(10), e0258889. https://doi.org/10.1371/journal.pone.0258889

Neumann, C. J., Grandel, H., Gaffield, W., Schulte-Merker, S., & Nüsslein-Volhard, C. (1999). Transient establishment of anteroposterior polarity in the zebrafish pectoral fin bud in the absence of sonic hedgehog activity. *Development*, *126*(21), 4817–4826. https://doi.org/10.1242/dev.126.21.4817

O'Meara, B. C., Ané, C., Sanderson, M. J., & Wainwright, P. C. (2006). Testing for different rates of continuous trait evolution using likelihood. *Evolution*, *60*(5), 922–933.

Olsen, A. M., & Westneat, M. W. (2015). StereoMorph: An R package for the collection of 3D landmarks and curves using a stereo camera set-up. *Methods in Ecology and Evolution*, *6*(3), 351–356. https://doi.org/10.1111/2041-210x.12326

Olson, E. C., & Miller, R. L. (1999). *Morphological integration*. University of Chicago Press.

Orkney, A., Bjarnason, A., Tronrud, B. C., & Benson, R. B. J. (2021). Patterns of skeletal integration in birds reveal that adaptation of element shapes enables coordinated evolution between anatomical modules. *Nature Ecology & Evolution*, *5*(9), 1250–1258. https://doi.org/10.1038/s41559-021-01509-w

Paradis, E., & Schliep, K. (2019). ape 5.0: An environment for modern phylogenetics and evolutionary analyses in R. *Bioinformatics*, *35*(3), 526–528. https://doi.org/10.1093/bioinformatics/bty633

Petit, F., Sears, K. E., & Ahituv, N. (2017). Limb development: A paradigm of gene regulation. *Nature Reviews Genetics*, *18*(4), 245–258. https://doi.org/10.1038/nrg.2016.167

R Core Team. (2022). *R: A language and environment for statistical computing*. *R Foundation for Statistical Computing*. https://www.R-project.org/

Rabosky, D. L., Chang, J., Title, P. O., Cowman, P. F., Sallan, L., Friedman, M., Kaschner, K., Garilao, C., Near, T. J., Coll, M., & Alfaro, M. E. (2018). An inverse latitudinal gradient in speciation rate for marine fishes. *Nature*, *559*(7714), 392–395. https://doi.org/10.1038/s41586-018-0273-1

Revell, L. J. (2024). phytools 2.0: An updated R ecosystem for phylogenetic comparative methods (and other things). *PeerJ*, *12*, e16505. https://doi.org/10.7717/peerj.16505

Sfakiotakis, M., Lane, D. M., & Davies, J. B. C. (1999). Review of fish swimming modes for aquatic locomotion. *IEEE Journal of Oceanic Engineering*, *24*(2), 237–252. https://doi.org/10.1109/48.757275

Sordino, P., van der Hoeven, F., & Duboule, D. (1995). Hox gene expression in teleost fins and the origin of vertebrate digits. *Nature*, *375*(6533), 678–681. https://doi.org/10.1038/375678a0

Sorenson, L. (2007). Examining morphological characteristics of triggerfish: A three-dimensional reconstruction of skeletal and muscular features of *Rhinecanthus rectangulus*. *Journal of Young Investigators*, *1*, 1. www.jyi.org/2007-february/2017/11/11/examining-morphological-characteristics-of-triggerfish-a-three-dimensional-reconstruction-of-skeletal-and-muscular-features-of-rhinecanthus-rectangulus

Sorenson, L., Santini, F., Carnevale, G., & Alfaro, M. E. (2013). A multi-locus timetree of surgeonfishes (Acanthuridae, Percomorpha), with revised family taxonomy. *Molecular Phylogenetics and Evolution*, *68*(1), 150–160. https://doi.org/10.1016/j.ympev.2013.03.014

Standen, E. M., & Lauder, G. V. (2005). Dorsal and anal fin function in bluegill sunfish *Lepomis macrochirus*: Three-dimensional kinematics during propulsion and maneuvering. *The Journal of Experimental Biology*, *208*(Pt 14), 2753–2763. https://doi.org/10.1242/jeb.01706

Turingan, R. G. (1994). Ecomorphological relationships among Caribbean tetraodontiform fishes. *Journal of Zoology*, *233*(3), 493–521. https://doi.org/10.1111/j.1469-7998.1994.tb05279.x

Wainwright, P. C., Bellwood, D. R., & Westneat, M. W. (2002). Ecomorphology of locomotion in labrid fishes. *Environmental Biology of Fishes*, *65*(1), 47–62. https://doi.org/10.1023/a:1019671131001

Walker, J. A., & Westneat, M. W. (2002). Kinematics, dynamics, and energetics of rowing and flapping propulsion in fishes. *Integrative and Comparative Biology*, *42*(5), 1032–1043. https://doi.org/10.1093/icb/42.5.1032

Webb, P. W. (1984). Form and function in fish swimming. *Scientific American*, *251*(1), 72–82. https://doi.org/10.1038/scientificamerican0784-72

Wimberly, A. N., Slater, G. J., & Granatosky, M. C. (2021). Evolutionary history of quadrupedal walking gaits shows mammalian release from locomotor constraint. *Proceedings Biological Sciences*, *288*(1957), 20210937. https://doi.org/10.1098/rspb.2021.0937

Wood, R. (2003). The ecological evolution of reefs. *Annual Review of Ecology and Systematics*, *29*(1), 179–206. https://doi.org/10.1146/annurev.ecolsys.29.1.179

Young, N. M., & Hallgrímsson, B. (2005). Serial homology and the evolution of mammalian limb covariation structure. *Evolution*, *59*(12), 2691–2704. https://doi.org/10.1111/j.0014-3820.2005.tb00980.x

Young, N. M., Wagner, G. P., & Hallgrímsson, B. (2010). Development and the evolvability of human limbs. *Proceedings of the National Academy of Sciences of the United States of America*, *107*(8), 3400–3405. https://doi.org/10.1073/pnas.0911856107

Zelditch, M. L., & Goswami, A. (2021). What does modularity mean? *Evolution & Development*, *23*(5), 377–403. https://doi.org/10.1111/ede.12390